AMINOXYL CATALYZED ELECTROCHEMICAL ETHANOL DETECTION:

DEVELOPMENT OF A NEW BREATHALYZER USING MOLECULAR CATALYSIS

A THESIS IN
Chemistry

Presented to the Faculty of the University
of Missouri-Kansas City in partial fulfillment of
the requirements for the degree

MASTER OF SCIENCE

by
MIKAYLA NOELLE MAYER

B.S. Chemistry, University of Missouri-Kansas City, 2020

Kansas City, Missouri
2021

AMINOXYL CATALYZED ELECTROCHEMICAL ETHANOL DETECTION: DEVELOPMENT OF A NEW BREATHALYZER USING MOLECULAR CATALYSIS

Mikayla Noelle Mayer, Candidate for the Master of Science Degree

University of Missouri – Kansas City, 2021

ABSTRACT

Blood alcohol concentration (BAC) is the indicator of alcohol intoxication, and its measurement has emerged as the most common analytical procedure requested by law enforcement. Due to its volatility, ethanol vapor can be detected in breath, and its vapor concentration is proportional to BAC. While portable breathalyzers have been designed for simple breath alcohol concentration detection, they are limited by high cost or the need for frequent recalibration. The first chapter of this thesis discusses the instrumentation used currently for alcohol detection, as well as the few recent attempts to improve the current methods of alcohol detection by adopting enzymatic detection methods. Although promising advancements have been made, the instability and high cost of enzymes prevent their commercial application.

Chapter three describes how the unique catalytic activity of the aminoxyl radical/oxoammonium redox couple toward alcohol oxidation was harnessed for fabrication of an electrochemical ethanol sensor for breath analysis with experimental details described in chapter two. Our functional sensing element consists of a screen-printed electrode in which the graphene oxide-based working electrode is modified with aminoxyl derivatives, of which 4-hydroxy-2,2,6,6-tetramethylpiperidine 1-oxyl benzoate (TMB) was the most efficient

derivative. Exposing this modified electrode to simulated breath that contains ethanol, while applying the required potential for oxidation of the aminoxyl radical, generates an electrocatalytic current proportional to the ethanol concentration in the breath. These simple, sensitive, durable, and inexpensive electrodes may contribute to the development of a single-use reliable ethanol sensor for personal or law enforcement applications.

The faculty listed below, appointed by the Dean of the School of Biological and Chemical Sciences, have examined a thesis titled "Aminoxyl Catalyzed Electrochemical Ethanol Detection: Development of A New Breathalyzer Using Molecular Catalysis," presented by Mikayla Noelle Mayer, candidate for the Master of Science degree, and certify that in their opinion it is worthy of acceptance.

Supervisory Committee

Mohammad Rafiee, Ph.D., Committee Chair

Department of Chemistry

Keith R. Buszek, Ph.D.

Department of Chemistry

Zhonghua Peng, Ph.D.

Department of Chemistry

CONTENTS

ILLUSTRATIONS

ACKNOWLEDGEMENTS

My most sincere gratitude is first and foremost extended to my advisor, Professor Rafiee at the University of Missouri-Kansas City, for the ways in which he has supported, encouraged, and guided me throughout my studies. He has consistently expressed confidence in my abilities to grow and succeed as a chemist, even when I felt that I was incapable. I know that I would not be here without his mentorship, and I cannot thank him enough for instilling in me a deeper passion and appreciation for scientific research.

I am deeply grateful to Professor Keith Buszek and Professor Zhonghua Peng for their willingness to support me in my thesis committee. Each of their insights and suggestions were invaluable during my defense and I cherish the encouragement that they have given me as a growing scientist.

I would like to thank the other members of the Rafiee research group, Buwanila Punchihewa, Matthew Mumau, Amber Cunningham, and others, for supporting me, listening to several hours of presentations over the course of my research, asking questions, and providing stimulating conversation and important feedback. I am also thankful to Dr. Kathleen Kilway, Ms. Asia Williams, and Mr. Silas Arnold for their constant assistance and support throughout my masters studies.

Finally, I thank my parents for their constant support and reassurance as I have pursued what I love. Though my mom could not be around throughout my masters studies, her words of encouragement have always and will always remain with me. I am eternally grateful to my husband – my best friend and confidant – for his unwavering support and love. My accomplishments would mean nothing without each of my loved ones and the light they bring to my life.

CHAPTER 1

INTRODUCTION AND BACKGROUND

1.1 Early Examples of Breathalyzers

Alcohol abuse is one of the major problems faced by society today, leading to behavioral issues and almost one-third of traffic related deaths in the United States.[1,2] Blood alcohol concentration (BAC) is the indicator of alcohol intoxication, and its measurement has emerged as the most common analytical procedure requested by law enforcement. Due to this ever-increasing demand by law enforcement and rising incidents of alcohol-related problems, the ability to measure BAC in real-time is desirable. Determining BAC in a complex matrix such as blood is difficult, and blood sampling is considered an invasive test. However, the volatility of ethanol allows for its vapors to be detectable noninvasively in the breath. Breath alcohol concentration (BrAC) is proportional to BAC, therefore, using this correlation which will be discussed in further detail later, BAC can be easily estimated.

The ability to measure BrAC opened the door to various innovations of noninvasive testing methods for the indirect determination of BAC. In 1927, William McNally created the first hand-held, single use device which indicated intoxication as ethanol-containing breath passed through a solution of potassium dichromate that would then change color (**Figure 1.1**).[3] The color change was the result of a well-known reaction in organic chemistry, where strong oxidants such as dichromate or permanganate oxidize ethanol. The amount of ethanol was proportional to the expansion of the color changing region in the breathalyzer tube, providing a basis for semi-quantitative analysis. However, this did not provide a numerical value for ethanol concentration in the breath and, consequently, blood. Thus, its imprecision limited its use to situations such as zero-tolerance testing.

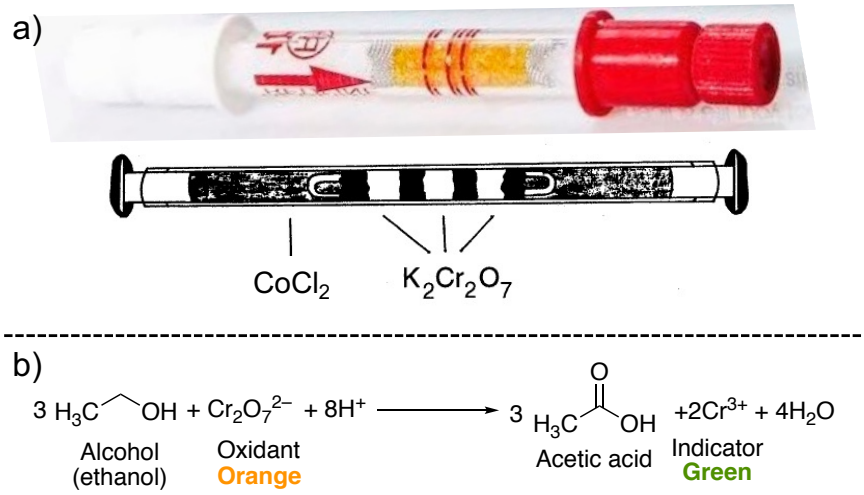

Figure 1. 1. Example of a single-use breathalyzer, Alcosense™ (a); chemical oxidation of ethanol via dichromate and associated color change (b).

The first practical roadside breathalyzer, the "drunkometer", was developed in 1931: the motorist's breath was collected in a balloon and subsequently pumped through a potassium permanganate solution. Any ethanol in the breath would induce a color change – the more intense the color change, the more ethanol present in the breath. Though unable to determine BrAC, these handheld breathalyzers highlighted the benefits of personal breathalyzers which would allow people to test themselves for intoxication before engaging in potentially dangerous activities such as driving.

1.2. Instrument Based Breathalyzer

To obtain more quantitative results, the color change needs to be encoded to produce a readable signal that corresponds to the concentration of ethanol (**Figure 1.2**). In 1954, Robert Borkenstein developed a breathalyzer which utilized photometry as the encoding method,

wherein light would pass through the solution where the chemical oxidation occurred, and the intensity of the light reflected was related to the concentration of ethanol in the solution. A spectrophotometer was necessary to read the absorbance in this situation and provide a quantitative value for the concentration of ethanol.

Figure 1. 2. Steps for developing a signal readout from a color changing chemical reaction, and the color change of dichromate after reduction by ethanol.

As demonstrated in Figure 1.2, the photometric technique relied on an absorbance change after a chemical reaction; however, certain spectroscopic techniques provide absorption peaks for ethanol that can be measured without a chemical reaction. As an organic molecule, ethanol has several bonds which are active in the infrared region. Infrared (IR) spectroscopy was utilized for ethanol detection beginning in 1954 and quickly became the most reliable method for quantitatively measuring BAC. The stretches of various types of bonds absorb IR radiation at specific wavelengths of light, producing a spectrum with peaks at those wavelengths. Additionally, the linear correlation of absorbance and concentration provides quantitative information on the concentration of ethanol in the sample (**Figure 1.3**).

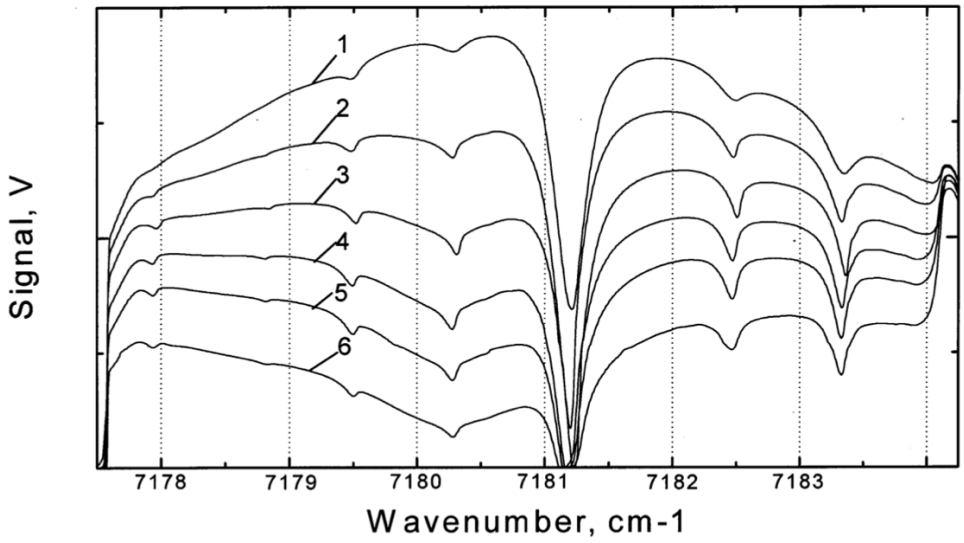

Figure 1. 3. Signal from a photodetector for various ethanol contents in 2-meter cell. (1–6-successive increasing of ethanol concentration from zero up to saturated vapor pressure). Adopted from ref 4.

Several IR-based devices for ethanol analysis have been developed since the 1980s, such as the Alcotest 7010, Breathalyzer 900, Intoximeter 3000, Intoxilyzer, and the most advanced device, DataMaster breath alcohol content verifier. Since then, many portable IR instruments have been fabricated and are currently used by law enforcement.[4] It is necessary to mention that absorption spectra of many organic molecules, including ethanol, are made up of several absorption bands, some of which are wide. Therefore, the absorption lines are positioned very close to each other and there is some possibility for overlap between the absorption bands of volatile organic compounds (VOCs) that exist in the breath. This possible interference highlights the option of using more advanced techniques like separation. Working with VOCs makes gas chromatography (GC) an ideal technique for breath analysis.

In GC, the sample is passed through a chromatographic column containing mobile and stationary phases: the stationary phase is fixed inside the column while the mobile phase, an

inert carrier gas, moves freely. The more similar a component is to the mobile phase, the quicker it will flow through the column. Thus, if ethanol-containing breath moves through the column at a specific temperature, ethanol will have a shorter retention time as compared to water due to its volatility. To determine the concentration of ethanol in the breath, however, a detector is needed. Mass spectrometry (MS) is often coupled with GC for this purpose – ethanol molecules are ionized, and the spectrometer measures the mass-to-charge ratio of the ions produced. This allows identification of not only ethanol, but also other volatile compounds in the breath. GC can also be coupled with IR, or numerous other types of detectors.

GC is a valuable analytical tool for its sensitivity and accuracy in providing quantitative information but presents some challenges. The initial cost of this instrument is high, sometimes more than $50,000, its maintenance is costly, and it needs to be operated by highly skilled personnel.[5] Figure 1.4 shows an example of a GC/MS instrument used for breath analysis.

Figure 1. 4. A comprehensive two-dimensional gas chromatography-mass spectrometer used for breath analysis. Adopted from ref 6.

GC/MS is a state-of-art analytical technique for the analysis of non-invasive exhaled VOCs, a potential method for early diagnosis of lung cancer and the health issues and diseases associated with alcoholic drink consumption.

One of the VOCs that exists in breath and is related to alcohol consumption is acetaldehyde.[6] Alcohol consumption is the major source of acetaldehyde exposure in individuals; it is produced in the liver from the metabolism of ethanol via the enzyme alcohol dehydrogenase (ADH) and is, in most cases, further oxidized to acetic acid via acetaldehyde dehydrogenase 2 (ALDH2). Deficiency of the ALDH2 enzyme, one of the most common genetic enzyme deficiencies, causes accumulation of acetaldehyde and results in tachycardia, headaches, and nausea. This deficiency affects 35%-40% of East Asians and 8% of the global population.[7] Numerous epidemiological studies have shown that although alcohol is not a carcinogen, alcohol consumption significantly increases risk for esophageal cancer; this conclusion was developed from multiple experimental models where acetaldehyde, the primary metabolite of ethanol, was proven to be carcinogenic.[8] Detection of acetaldehyde using full breath analysis techniques such as GC/MS is possible due to the extremely volatile nature of the compound.

The size and condition for operation prevents GC from being a portable device for on-site use, therefore it is currently only used in the laboratory and in further legal appeals.[9,10] On-site analysis is beneficial to law enforcement, but has imperative application particularly in healthcare where point-of-care detection is valuable. Point-of-care devices allow medical testing at or near the point of care by healthcare professionals, providing real-time monitoring. An example of point-of-care testing is measuring the blood sugar (glucose) levels in diabetic patients, which will be described in further detail later in section 1.3.

1.3. Electrochemical Breathalyzers

In the early 1970s, Tom Parry Jones proposed and began to examine the possibility of using a small fuel cell for measuring BrAC, where ethanol oxidation at the surface of a platinum-based electrode is the anodic reaction (**Figure 1.5**).[11] The anodic current is directly proportional to the alcohol content of the breath with no need for additional detectors, unlike spectroscopic techniques. This advantage facilitated the possibility of miniaturization, turning this electrochemical breathalyzer into the first example of a handheld breathalyzer.

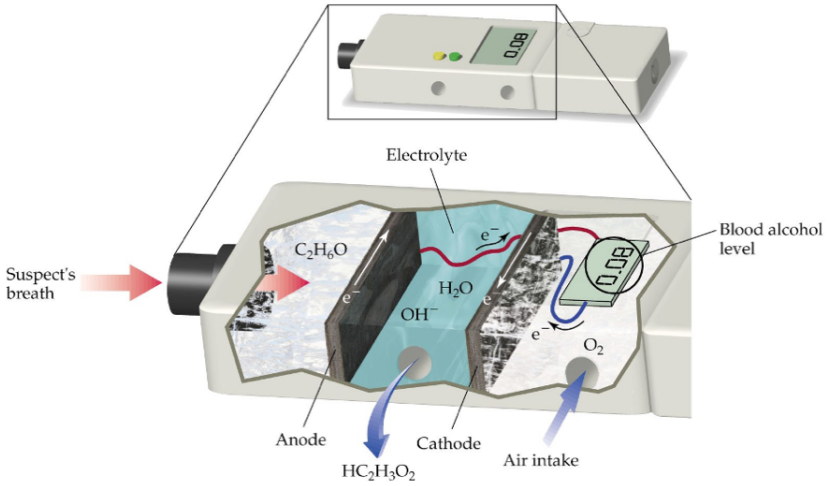

Figure 1. 5. Schematic of a handheld electrochemical breathalyzer, adopted from ref 12.

The high cost of platinum that is used for the anode (sensing element) brings a disadvantage to this breathalyzer. The anode cannot be displaced after each use and is integrated with other parts of the breathalyzer, preventing the utilization of single-use electrodes. Multiple uses of the breathalyzer and electrode causes a memory effect from previous uses; therefore, to have a reliable signal, it needs frequent calibration. Further, a recent study by Allan and coworkers highlighted the negative effect of humidity on the sensing

performance of these commercially available breathalyzers.[12] Consequently, the electrochemical breathalyzers do not provide reliable enough results to be used as evidence in court and more advanced techniques are needed such as the previously discussed IR spectroscopy or GC.

One example of an electrochemical sensor with a single-use and disposable sensing element is the sensor used for monitoring blood sugar (glucose). These sensors are used worldwide as portable, even wearable, devices for continuous glucose monitoring. Glucose monitors are based on electrochemical enzymatic detection, wherein the analyte (glucose) binds to a bioreceptor (e.g., glucose oxidase) which oxidizes glucose in the presence of oxygen, producing hydrogen peroxide. Hydrogen peroxide is then oxidized by Prussian blue, providing an electrical signal which can be sent wirelessly to a monitor that gives a simple readout to the user. One commercially available miniaturized, wearable glucose sensor provides continuous monitoring of glucose in interstitial fluid without the invasiveness of finger pricking, though the sensor needs to be replaced every few days for accurate results. The device communicates the results to a smartphone, which can be transmitted to a healthcare professional, similarly to older versions of glucose monitors that require a blood sample for testing. Thus, it quickly became one of the most successful examples of point-of-care diagnostics. The lack of a of single-use electrode for currently available breathalyzers prevent its global and commercial utility, as seen with blood glucose meters. There have been limited attempts, described in section 1.4, at producing disposable sensing elements based on the electrocatalytic oxidation of alcohol.

1.4 Recent Developments in Electrocatalytic Detection of Ethanol

The similarity of functional groups for ethanol and glucose, as both have primary hydroxyl groups, became the basis for transforming the glucose sensors to ethanol sensors, using enzymes specific to ethanol. For example, Pingarrón and coworkers investigated an enzymatic pathway for the detection of alcohol in sweat via electrocatalytic oxidation (**Figure 1.6**).[13] The group fabricated a graphite-Teflon-AOD-HRP-ferrocene composite electrode for the detection of ethanol. As sweat is induced, ethanol is oxidized by the enzyme alcohol oxidase (AO) in the presence of oxygen, producing hydrogen peroxide. The second enzymatic cycle using horseradish peroxidase (HRP), mediated by ferrocene, monitors the entire process at low potential (0.00V) vs. the Ag/AgCl reference electrode. The amperometric signal generated through ferricinium reduction is proportional to the ethanol content in blood, allowing for both continuous and isolated monitoring of BAC. Although the system detects ethanol rapidly, it takes several minutes for a steady state to be achieved. Additionally, the use of multiple enzymes decreases its overall stability and requires it to be stored in specific conditions for reliable results.

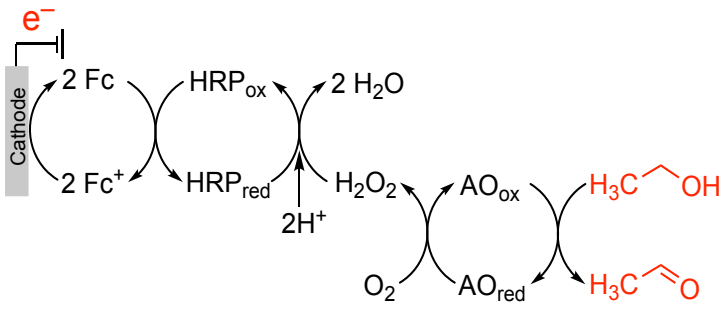

Figure 1. 6. Enzyme and electrode reactions involved in the response of graphite-Teflon-AOD-HRP-ferrocene composite electrodes to alcohol.

Shortly following, Wang and coworkers developed a flexible, wearable tattoo-based biosensor for alcohol detection.[14] Ethanol in the sweat is detected in a similar manner as that of Pingarrón and coworkers using AO; however, the group simplified the catalytic pathway by replacing the electron mediator, ferrocene, and HRP with Prussian blue (PB), a highly efficient compound for facilitating electron transfer (**Figure 1.7**). The device can be wirelessly connected to a smartphone, allowing the user to easily view his/her own drinking level. The group showed that ethanol sensing elements could be miniaturized. However, detection time is relatively long and due to the use of the enzyme, the device has low stability over time.

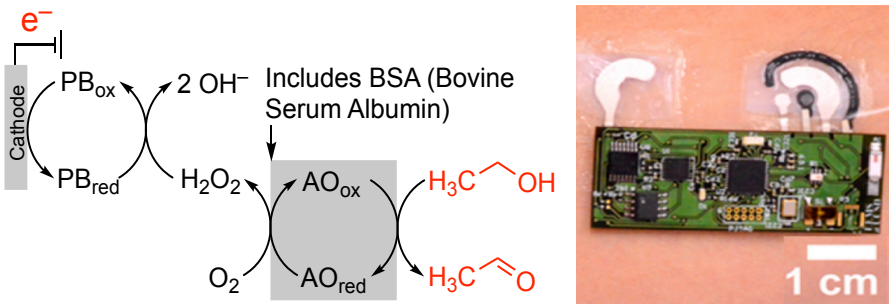

Figure 1. 7. Enzyme and electrode reactions involved in the amperometric sensing of ethanol in sweat on a wearable tattoo-based biosensor.

Even more recently, a paper-based breathalyzer was introduced by Bihar and coworkers in which alcohol dehydrogenase (ADH) catalyzes ethanol oxidation by nicotinamide adenine dinucleotide (NAD^+).[15] This detection system is paired with an organic electrochemical transistor (OECT), made with the polymer poly(3,4-ethylenedioxythiophene):poly(styrenesulfonate) (PEDOT:PSS), to correlate ethanol concentration and conductivity. The collected electrons from this ethanol oxidation transfer to the OECT and cause the reduction of polyethylenedioxythiophene (PDT^+). Reduction of the

cationic functional groups changes the conductivity of the polymer, which conductivity change has shown to be proportional to the alcohol content of breath. This group effectively demonstrated a proof-of-concept for a breathalyzer using a disposable, paper-printed sensing element (**Figure 1.8**).

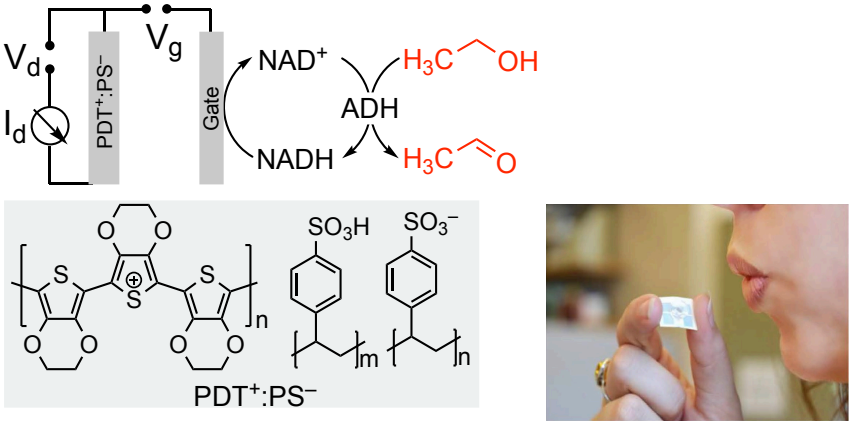

Figure 1. 8. Enzymatic reaction of ethanol and ADH in electrolyte solution, where ethanol is oxidized to acetaldehyde, and NAD^+ is reduced to NADH. Breathing on the printed PEDOT:PSS OECT allows for alcohol detection.

Each of these important examples proved that the detection system for ethanol in sweat or in the breath could be miniaturized and easily fabricated. However, their main barriers for commercialization lie in the fact that they are based on enzymatic alcohol oxidation. While enzymes are desirable for their selectivity and specificity towards certain reactions, their durability, cost, and required conditions for enzymatic reactions create problems for practical use.

1.5 Aminoxyl-Catalyzed Alcohol Oxidation

Aminoxyl compounds, categorized by the general structure $R_2N–O•$ (R=alkyl), exemplify a versatile class of organic radical reagents possessing distinctive properties and reactivity. Due to their diverse chemistry, *N*-oxyl compounds have been utilized in numerous applications including use as antioxidants in biological studies, charge carriers for energy storage, spin labels in electron spin resonance (ESR) studies, mediators in polymerization reactions, and catalysts in chemical and electrochemical oxidation reactions.[16] A representative example of aminoxyl radicals is 2,2,6,6-tetramethylpiperidine *N*-oxyl (TEMPO). Its highly substituted sites adjacent to the *N*-oxyl group contribute to its stability, making TEMPO a stable radical under ambient conditions. Persistent aminoxyl radicals display unique redox properties that play a significant role in their reactivity. Reduction of TEMPO gives the corresponding hydroxylamine (TEMPOH), and its oxidation results in the formation of the oxoammonium ($TEMPO^+$) (**Figure 1.9**). This oxoammonium species serves as an oxidant in numerous organic oxidation reactions.

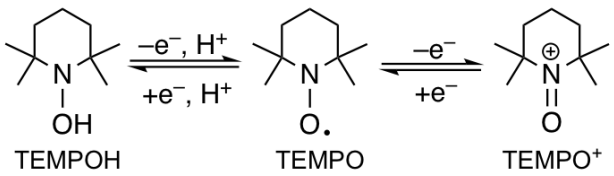

Figure 1. 9. Electron transfer of the aminoxyl radical, TEMPO.

One example of an organic reaction facilitated by an aminoxyl radical is alcohol oxidation, first reported by Golubev, in which stoichiometric amount of $TEMPO^+$ was used.[17] Since then, cyclic aminoxyl species have found extensive use as reagents for the oxidation of

alcohols to the corresponding aldehydes, ketones, and carboxylic acids.[16] Later, the reaction was modified by using the TEMPO in catalytic amount and low-cost chemical oxidants like bleach.[18] Studies have shown there are two possible mechanisms for alcohol oxidation by $TEMPO^+$. The first is observed under basic conditions in which the alkoxide form of alcohol forms an adduct with $TEMPO^+$ to generate TEMPOH and the oxidized product (aldehyde or ketone). The TEMPOH turns to $TEMPO^+$ in the presence of excess terminal oxidants (like bleach) (**Figure 1.10**, top pathway). Under acidic conditions the mechanism is proposed to involve bimolecular hydride transfer between electron rich alcohol and electron deficient $TEMPO^+$ to generate the same products (**Figure 1.10**, bottom pathway).

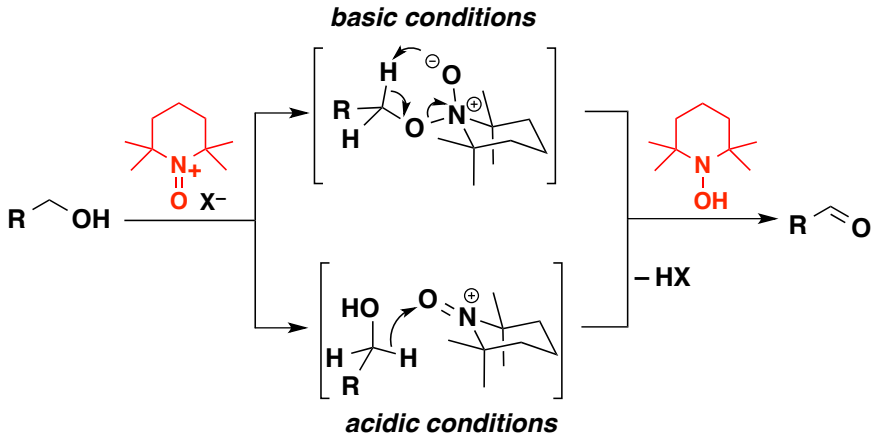

Figure 1. 10. Mechanism for TEMPO catalyzed alcohol oxidation in basic and acidic conditions. Adopted, with modifications, from ref 23.

The reactions under basic conditions are typically considerably faster than those under acidic conditions, making them the most established and utilized mechanism for aminoxyl catalyzed alcohol oxidation.[19,20] Due to the reversible electron transfer of many aminoxyls, electrochemical oxidation of alcohols became an alternative to chemical oxidation methods. In

1983, Semmelhack and co-workers reported the first use of an aminoxyl radical as an electrocatalyst for alcohol electrooxidation and examined certain mechanistic aspects of this reactivity.[21] The reaction between electrogenerated $TEMPO^+$ with alcohols in the presence of base (like 2,6-lutidine) was found to be fast and significantly fast catalytic turnovers were achieved. This continual turnover and reoxidation of TEMPOH, regenerated by alcohol oxidation, produces a significant enhancement of current under electrochemical conditions.

In 1996, Ohmori and co-workers used this current enhancement, with cyclic voltammetry (CV) as an electroanalytical tool, to examine the rate and mechanism of TEMPO catalyzed alcohol oxidation under basic conditions.[22]

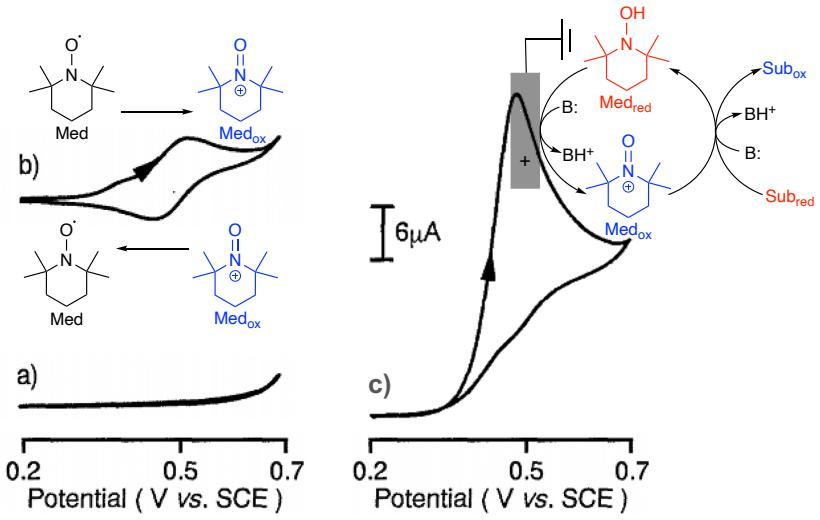

Figure 1. 11. Cyclic voltammograms of background current (a), TEMPO (b), and the catalytic activity of TEMPO in the presence of electrochemically inactive substrate (c). Adopted, with modifications, from ref 16.

The cyclic voltammogram of TEMPO shows an anodic peak corresponding to the oxidation of TEMPO to $TEMPO^+$ (demonstrated as Med and Med_{ox} in **Figure 1.11b**), and subsequently a cathodic peak on the reverse scan which corresponds to the reduction of electrochemically

generated $TEMPO^+$ to TEMPO. In the presence of alcohol, increase in the anodic peak current and disappearance of the cathodic peak current (**Figure 1.11c**) are characteristics of a catalytic electrochemical-chemical pathway, known as EC′. In an oxidative EC′ reaction, the reduced mediator, Med_{red}, undergoes an electrochemical oxidation (E) to generate Med_{ox}, which then undergoes a chemical redox reaction (C′) with the reduced substrate, Sub_{red}, to generate Sub_{ox} and Med_{red} . Consumption of Med_{ox} in the chemical step results in the lack of a cathodic peak, and regeneration of Med_{red} in the chemical reaction and its oxidation at the electrode surface causes enhancement in anodic peak current. It should be noted that the alcohol itself which is the substrate here (Sub_{red}) is not electroactive at this potential range.

The enhancement of the oxidation peak current is proportional to the turnover number (TON) of the catalytic cycle and can be utilized to evaluate the catalytic activities of various aminoxyls. For example, a study by Stahl and co-workers compares the catalytic behavior of 9-azabicyclo[3.3.1]nonane *N*-oxyl (ABNO) with that of the TEMPO derivative, 4-acetamido-TEMPO (ACT) in the presence of 1-butanol (**Figure 1.12**).[23]

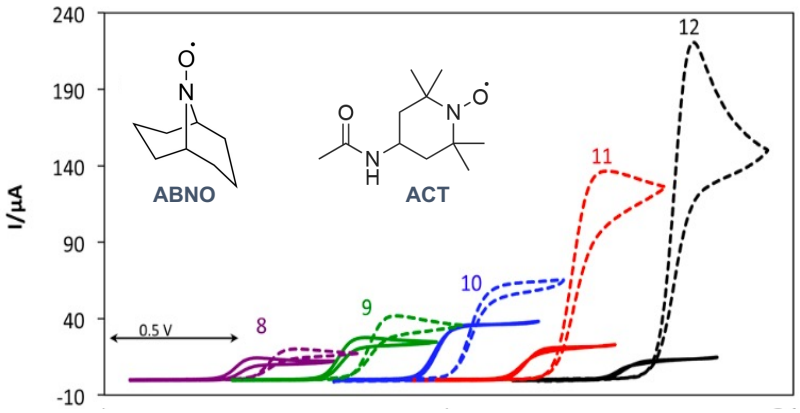

Figure 1. 12. Cyclic voltammograms of ABNO (solid line) and ACT (dashed line) in the presence of 50 mM 1-butanol at various pH values, scan rate 50 mV s^{-1}. Adopted, with modifications, from ref 23.

The cyclic voltammograms show the higher electrocatalytic activity of ACT toward this primary alcohol, indicated by the significantly higher current observed for ACT compared to ABNO. Additionally, the expected trend of catalytic activity in increasingly basic conditions is not observed for ABNO. Two important parameters that affect the reactivity are steric hinderance and redox potential of aminoxyl radicals. The study by Stahl and co-workers highlights that increased driving force (i.e., higher redox potential) can surmount steric effects in promoting the catalytic activity of aminoxyls. Understanding the structural differences between aminoxyls and the ways in which those features affect their reactivity is essential in selecting an electrocatalyst. Sigman and co-workers demonstrated that destabilization of both the oxoammonium form and, more importantly, the hydroxylammonium form of aminoxyls increases their catalytic activity.[24] Adding a permanent ammonium cation to the structure, for example, destabilizes the hydroxylammonium because of the repulsion between the two cations within proximity. Destabilization can also be achieved through geometric modifications, such as using a polycyclic catalyst. The decreased buildup of hydroxylammonium lowers the oxidation potential for regeneration of the oxoammonium, resulting in significantly higher catalytic activity. This concept allows for considerable variability in aminoxyl structure which means they can be tailored to the desired reaction and grouped according to their sterics and redox potential (**Figure 1.13**).

Aminoxyl compounds have been extensively used as catalysts and co-catalysts with chemical oxidants, such as bleach, for application in organic synthesis including synthesis of pharmaceuticals.[18,25] Electrochemical study of the aminoxyl catalyzed alcohol oxidation not only draws attention to the elimination of chemical oxidants but also highlights a contrast between the use of electrochemical versus chemical methods for reoxidation of the catalysts

during the reaction. Under chemical conditions, the catalyst turnover is limited by the fixed oxidation potential of oxidant. Under electrochemical conditions, however, the oxidation rate is normalized by adjustment of the applied potential. This concept has been used for classification of various aminoxyl compounds for different applications, including catalytic oxidations.

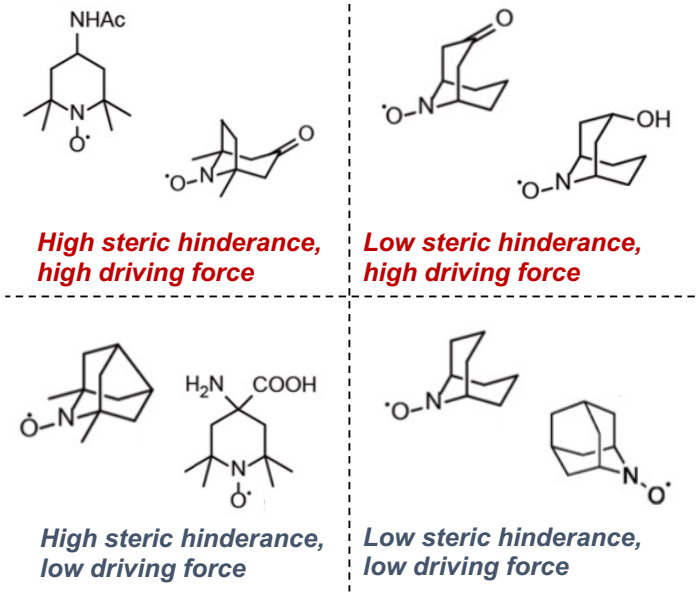

Figure 1. 13. Categorization of some aminoxyl compounds based on structural differences.

The powerful catalytic activity of enzymes combined with their electrochemical activities made electrochemical detection one of the traditional strategies for bioanalytical sensing.[26] The discussion above provides evidence of the similarities between the electrochemical and catalytic activity of aminoxyl compounds and enzymes for electrochemical detection of organic molecules and biomolecules such as ethanol. Relatively low redox potentials of aminoxyls and mild conditions can exclude them from the group of typical nonselective chemical catalysts that work under harsh conditions.

There are a few examples of using these advantages for electrocatalytic oxidation of alcohols. For example, in a study by Kashiwagi and coworkers, the aminoxyl nortropine-*N*-oxyl (NNO) was shown to effectively oxidize choline and other alcohols in physiological conditions with an ideal catalytic activity and selectivity (**Figure 1.14**).[27] The difference in catalytic current of NNO for oxidation of different alcohols highlights the potential selectivity even for the same functional group in different molecules. Figure 1.14 shows the order of reactivity for oxidation is D-glucose > choline > L-lactate and the rate of L-lactate oxidation is negligible compared to the other two alcohols.

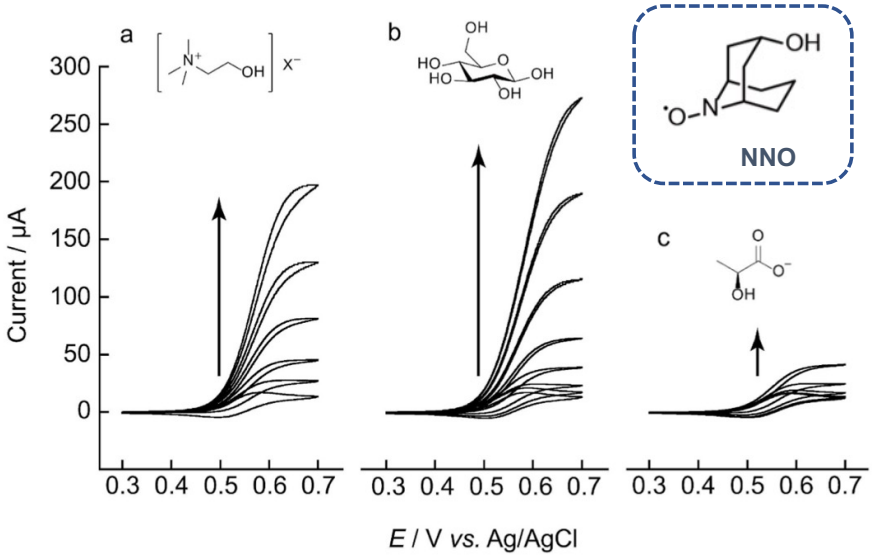

Figure 1. 14. Cyclic voltammograms of NNO (1.0 mM) in the absence and presence of 1.0, 3.0, 10, 30, 100 mM choline (a), D-glucose (b) and L-lactate (c) in 100 mM phosphate buffer solution (pH 7.4). The scan rate was 100 mV s^{-1}. Adopted, with modifications, from ref 27.

In an earlier work, Kashiwagi and co-workers reported the possibility of chiral discrimination for two alcohol enantiomers using a chiral aminoxyl compound. They used (6*R*,7*S*,10*R*)-4-oxo-2,2,7-trimethyl-10-isopropyl-1-azaspiro[5.5]undecane-*N*-oxyl (TIANO)

as a chiral catalyst that displayed higher catalytic activity in the presence of (*R*)-1-phenylethanol as compared to its (*S*)-isomer (**Figure 1.15**). The TEMPO derivative was used for the detection of (*R*) in an excess amount of (*S*)-isomer.[28]

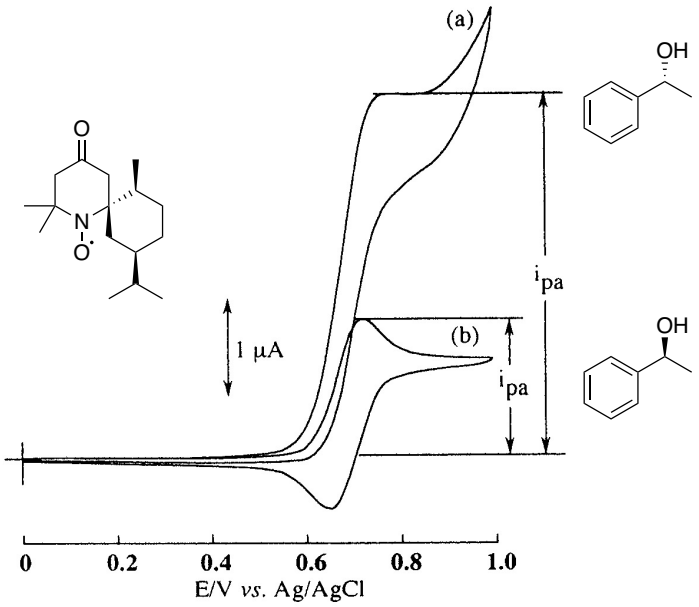

Figure 1. 15. Cyclic voltammograms of TIANO (0.1 mM) in $NaClO_4/CH_3CN$ (0.1 M) in the presence of (*R*)- 1.6 mM (a) and (*S*)-1-phenylethanol 1.6 mM (b). The sample solution contains 2,6-lutidine (3.2 mM). Scan rate: 25 mV s^{-1}. Adopted, with modifications, from ref 28.

In this project, we will utilize the well-defined redox reactions and structure-dependent catalytic activity of the aminoxyl compounds for ethanol oxidation in the gas phase and development of a new electrochemical system for ethanol detection in the breath. The project will be initiated by voltammetric and chronoamperometric studies of the electrocatalytic oxidation of ethanol by a variety of aminoxyl radicals in the presence of different bases. The sensing element will be a screen-printed carbon electrode where its working electrode is

modified with aminoxyl radicals and base or a paste including these components. The modified electrode (sensing element) will be exposed to simulated breath with different alcohol contents while the required potential for generation of oxoammonium is applied. The current generated from catalytic ethanol oxidation is proportional to ethanol concentration, providing a measure for quantification of ethanol content in breath. Electrode modification techniques include: a) deposition of a carbon paste containing different graphene and graphene oxide materials, and b) drop casting the mixture of aminoxyl radical and base on the surface of a commercially available graphene oxide based screen-printed electrode.

CHAPTER 2

EXPERIMENTAL

2.1 General Details

All solvents and chemicals were attained from commercial suppliers and used without any purification. Voltammetric and chronoamperometric experiments were conducted utilizing NuVant EZstat potentiostat/galvanostat and DropSens multichannel potentiostat/galvanostat. For homogeneous studies in aqueous phase, a 10 mL Pine electrochemical cell was utilized and equipped with a Ag/AgCl (internal solution 3 M KCl) reference electrode, a Pt wire counter electrode, and a glassy carbon disk (2 mm) as the working electrode. For electrochemical studies in gas phase and some of the electrochemical studies in aqueous phase, screen-printed electrodes (SPEs) from DropSens were utilized. SPEs are made by printing different kinds of ink on a plastic strip (**Figure 2.1**).

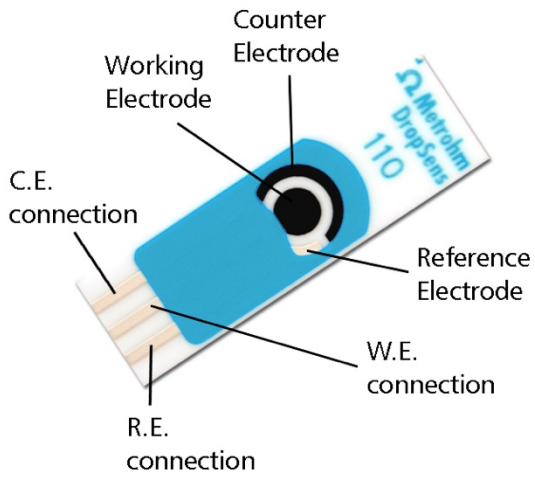

Figure 2. 1. Picture of a screen-printed electrode (SPE) used for these studies. W.E., R.E., and C.E. are abbreviations of working, reference, and counter electrodes, respectively.[29]

The SPEs that were used in these studies were fabricated with a Ag/AgCl ink as reference electrode due to its stable electrochemical potential under various measurement conditions, and a carbon ink as counter electrode. A variety of SPEs are available based on their working electrode materials; we utilized carbon–, carbon nanotube–, and graphene oxide–based working electrodes to conduct our experiments. The working electrodes had a 3 mm diameter. The electrode has three individual connections that can be inserted into an adapter connected to the potentiostat.

2.2 Experimental Procedures

2.2.1 Homogeneous Catalyst Studies

For the homogeneous studies in solution phase, a 10.0 mM stock solution of the aminoxyl catalyst was prepared by dissolving the desired amount of catalyst in aqueous or acetonitrile (MeCN) solvents. A 10 mL solution was prepared in the electrochemical cell by mixing 1 mL catalyst stock solution and 9 mL stock solution of supporting electrolyte and/or base and analyzed by cyclic voltammetry (CV) or chronoamperometry (CA). For 4-hydroxy-2,2,6,6-tetramethylpiperidine *N*-oxyl benzoate (TMB) catalyst, instead of 9 mL stock solution of supporting electrolyte, 7 mL of these solutions and 2 mL MeCN was utilized to ensure dissolution of this hydrophobic organic compound.

The stock solutions of catalysts and supporting electrolyte and/or base are:

- 10 mL 2,2,6,6-tetramethylpiperidine *N*-oxyl benzoate (TEMPO) (0.0156 g, 0.100 mmol) in D.I. water
- 10 mL TMB (0.0276 g, 0.100 mmol) in MeCN
- 10 mL 9-azabicyclo[3.3.1]nonane *N*-oxyl radical (ABNO) (0.0140 g, 0.100 mmol) in D.I. water
- 500 mL NaCl by dissolution of 5.8 g NaCl in D.I. water
- 500 mL sodium acetate (NaOAc) by dissolution of 8.2 g NaOAc in D.I. water
- 500 mL sodium bicarbonate ($NaHCO_3$) by dissolution of 8.4 g $NaHCO_3$ in D.I. water
- 500 mL sodium carbonate (Na_2CO_3) by dissolution of 10.6 g Na_2CO_3 in D.I. water
- 500 mL $NaHCO_3$/Na_2CO_3 buffer (0.1 M each) by mixing 1:1 stock $NaHCO_3$ and Na_2CO_3.

For voltammetric analysis after the initial potential screening and seeing the oxidation and reduction peaks, the potential range was adjusted, ideally between 350 mV less than reduction peak potential and 350 mV more than oxidation peak potential. For the CA experiment the potential was adjusting at 100 – 150 mV more positive to the oxidation peak potential of the catalyst (determined from CV experiment) for the desired amount of time, typically 5 to 20 seconds.

The desired amount of ethanol was added to the catalyst-only solution in the electrochemical cell, following examination of the catalyst itself, to ensure the most accurate comparison between the cyclic voltammograms or chronoamperograms before and after its addition. For example, 30 μL for a 50 mM solution was added using a 10-100 μL micropipette.

2.2.2 Fuel Cell Type Assembly

Ideal conditions for polymerization of polyaniline (PANI) were determined using a glassy carbon electrode. A supporting electrolyte stock solution of 0.1 M H_2SO_4 was prepared by adding 0.55 mL H_2SO_4 to a 100-mL volumetric flask and diluting to the mark with D.I. water. A solution of 0.1 M aniline in 0.1 M H_2SO_4 was prepared by adding 100 μL aniline to 10 mL H_2SO_4. To the electrochemical cell, 0.5 mL of aniline in H_2SO_4 were added to 9.5 mL stock 0.1 M H_2SO_4. To generate PANI at the surface of glassy carbon, the potential was scanned from 0–1.2V using CV for five cycles. The working electrode was then placed into a 10-mL solution of only 0.1 M H_2SO_4 to ensure the presence of PANI on the electrode surface.

For electrochemical deposition of PANI onto the graphite piece, a “working electrode” was assembled using a half cylinder piece of graphite and a half cylinder piece of PEEK with a cut-out down the middle. Nafion membrane was placed between the two half cylinders and

a piece of copper foil was placed on the outer surface of the graphite piece; the entire electrode was sealed using heat shrink tubing. Both ends of the graphite were covered with non-conductive glue to ensure PANI would only deposit onto the center of the graphite piece. Electrochemical polymerization was conducting via CV in the same manner as with the glassy carbon electrode.

For fabrication of the catalyst ink to use on the working electrode, the catalyst, TMB (0.005 g), was dissolved in 0.20 mL MeCN in a small glass vial. To the vial was added 0.20 mL 10% Nafion dispersion in water, 0.60 mL 0.2 M Na_2CO_3, and 0.02 g graphene nanoplatelets; the entire contents were stirred. Using a 10 µL micropipette, the ink was deposited onto the surface of several graphite electrodes. Each was allowed to dry 2 h. The electrodes were examined in NaCl and Na_2CO_3 supporting electrolyte solutions, without and with the desired amount of ethanol.

2.2.3 Screen Printed Electrodes in Aqueous Conditions

For the catalyst studies on SPEs in aqueous conditions, stock solutions of the catalysts without and with 500 mM EtOH were prepared:

- 10 mL TEMPO (0.0156 g, 0.100 mmol) in MeCN
- 10 mL TEMPO and 0.307 mL EtOH in MeCN
- 10 mL 4-acetamido-TEMPO (ACT) (0.0213 g, 0.100 mmol) in MeCN
- 10 mL ACT and 0.307 mL EtOH in MeCN
- 10 mL TMB (0.0276 g, 0.100 mmol) in MeCN
- 10 mL TMB and 0.307 mL EtOH in MeCN.

The final solutions were made by mixing 20 µL catalyst (or catalyst + EtOH) solution, 90 µL 0.2 M $NaHCO_3$, and 90 µL 0.2 M Na_2CO_3 in small glass vials. Using a 10 µL micropipette, the solutions were deposited onto the surface of several SPEs.

2.2.4 Generation of Simulated Breath with Ethanol Content

For generation of a mixture of ethanol, air, and water similar to the breath, the setup in Figure 2.2 was utilized, in which the gas washing bottles were filled with water or aqueous solutions of ethanol with the following concentrations:

- 60 mM EtOH (by dissolution of 1.84 mL EtOH in 500 mL D.I. water)
- 135 mM EtOH (by dissolution of 4.15 mL EtOH in 500 mL D.I. water)
- 200 mM EtOH (by dissolution of 6.15 mL EtOH in 500 mL D.I. water)

Considering the amount of water in the breath (which has 100% relative humidity) and the BrAC to BAC ratio of 1/2000 at human body temperature, the above-mentioned concentrations give the simulated breath corresponding to 0.036%, 0.080%, 0.119%, and 0.178% BAC, respectively.[30] It should be noted that the BAC value of 0.080% is the federal limit to legally drive in the United States. A gas tank was used for bubbling air through the gas washing bottles.

To obtain the most accurate comparison of cyclic voltammograms and chronoamperograms before and after exposure to EtOH, the SPEs were first exposed to only water vapor for about 15 seconds. All solutions were maintained at 37°C while testing the SPEs using a warm water bath. Schematic presentation of the setup and its picture are shown in Figure 2.2 and 2.3, respectively.

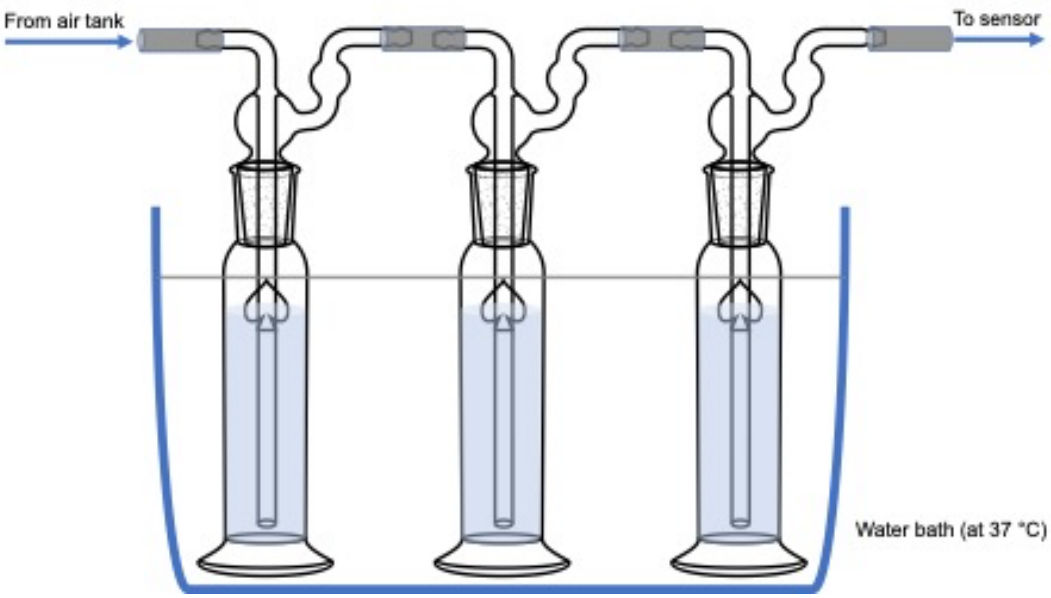

Figure 2. 2. Schematic presentation of the setup for generation of simulated breath.

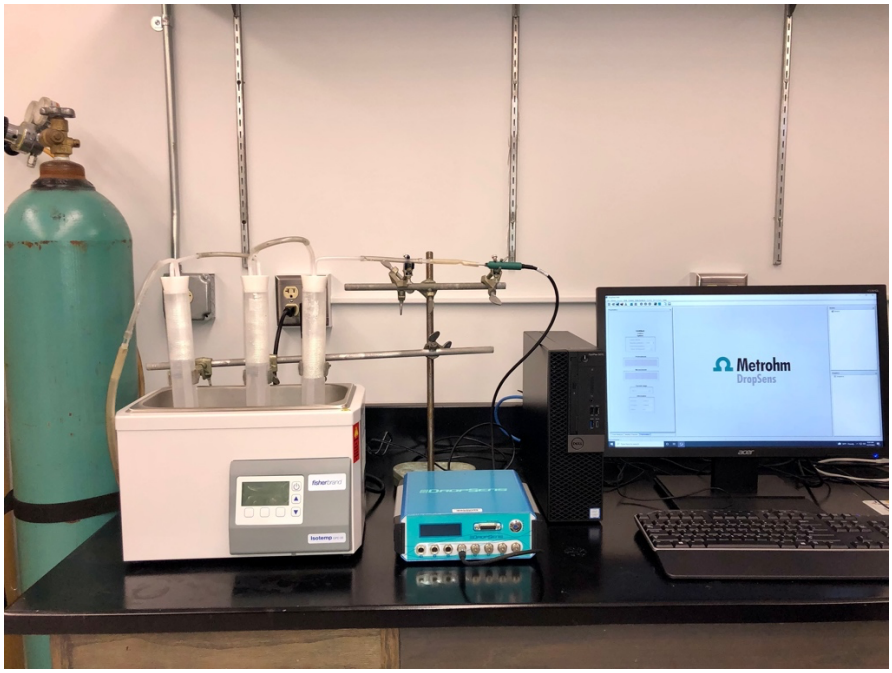

Figure 2. 3. Setup for gas phase studies using SPEs, including potentiostat with SPE connection, computer with DropSens software, nitrogen gas tank, and water bath containing gas washing bottles.

2.2.5 Carbon Paste Electrodes

To fabricate the carbon paste, a specified amount of catalyst was ground to a fine powder using a mortar and pestle. The desired carbon materials (listed below) were mixed with the catalyst powder and paraffin oil was added until the proper paste consistency was obtained. The catalysts examined were ABNO and TMB. Catalyst loading varied from 1, 2.5, and 5 mg in the paste. The optimized amount of paraffin oil and carbon-based materials are listed below.

- 0.2000 g graphene (G) and 0.2600 g paraffin oil with 0.0050 g catalyst
- 0.1750 g G, 0.2600 g paraffin oil, and 0.0250 g $NaHCO_3$ with 0.0050 g catalyst
- 0.0600 g basic graphene oxide (BGO) and 0.0460 g paraffin oil with 0.0025 g catalyst
- 0.0300 g each of G and BGO and 0.0560 g paraffin oil with 0.0025 g catalyst.

The amount of paraffin oil was adjusted slightly when adding different amounts of catalyst or when adding solid or liquid bases to the paste. The carbon pastes were placed on either the surface of a graphite electrode for aqueous studies or on the working electrode of a SPE for gas phase studies.

To make BGO for the carbon pastes, graphene oxide (GO) was treated with NaOH. Based on the reported value for oxygenated functional groups on GO (~11%), there should be about 0.105 g oxygen (6.56 mmol) in a 0.95 g sample of GO, and 3.28 mmol carboxylic acid functional groups. Thus, the carboxylic acid groups in a 1 g sample of GO can be deprotonated by about 3.0 mL of a 0.1 M NaOH solution. A 1 M solution of NaOH was first prepared by dissolution of 0.4024 g NaOH in 10 mL D.I. water. GO (0.3000 g) was added to 1 mL of 1 M NaOH in a small vial and the mixture was stirred for 30 minutes. After stirring, the vial was transferred to an oven under vacuum to completely dry the BGO.

2.2.6 Graphene Oxide Screen-Printed Electrodes

Solutions of varying concentrations of NaOH were prepared for treatment of graphene oxide screen-printed electrodes (GOSPEs):

- 0.10 M NaOH by dissolution of 0.4000 g NaOH in 100 mL D.I. water
- 0.04 M NaOH by dilution of 4 mL 0.1 M NaOH in 10 mL D.I. water
- 0.01 M NaOH by dilution of 1 mL 0.1 M NaOH in 10 mL D.I. water.

To treat the GOSPEs, 10 μL of the desired NaOH solution were drop cast onto the working electrode area of the GOSPEs and the electrodes were allowed to dry.

To prepare the catalyst solution, a stock solution of paraffin oil in ethyl acetate (EtOAc) was prepared by dissolution of 1.0000 g paraffin oil in 25 mL EtOAc. The catalyst solutions with different catalyst loading were made by mixing the following:

- TMB (0.0020 g) in 2.0 mL paraffin oil in EtOAc
- TMB (0.0050 g) in 2.0 mL paraffin oil in EtOAc
- TMB (0.0150 g) in 2.0 mL paraffin oil in EtOAc.

Following base treatment, 2 μL of the desired catalyst solution was drop cast onto the working electrode area of the GOSPEs and set aside so the EtOAc could evaporate off the electrode. Base optimization was carried out using the solution bearing 5 mg TMB for the most accurate comparison between electrodes.

CHAPTER 3

RESULTS AND DISCUSSION

3.1 Voltammetric Study of Aminoxyl Catalyzed Ethanol Oxidation in Solution

Our study was initiated with voltammetric examination of catalyst stability and reactivity toward ethanol oxidation in liquid phase. The reversibility of an electron transfer process can be determined through study of the aminoxyl via cyclic voltammetry. One of the aminoxyl compounds that we studied was 4-hydroxy-2,2,6,6-tetramethylpiperidine *N*-oxyl benzoate (TMB), where previous studies have shown that it is the most reactive aminoxyl catalyst for alcohol oxidation.[23] The cyclic voltammogram of a 1.0 mM TMB solution under mildly basic conditions, 0.2 M aqueous $NaHCO_3$ solution, shows an anodic peak in scanning to more positive potentials for oxidation of TMB to its oxoammonium (TMB^+), and subsequently a cathodic peak, on the reverse scan, which corresponds to the reduction of electrochemically generated TMB^+ to TMB (**Figure 3.1**). The ratio between the cathodic peak current and the anodic peak current (i_{pc}/i_{pa}) is unity, and the peak-to-peak separation (E_{pa}-E_{pc}) is approximately 60 mV, indicating a reversible electron transfer process.

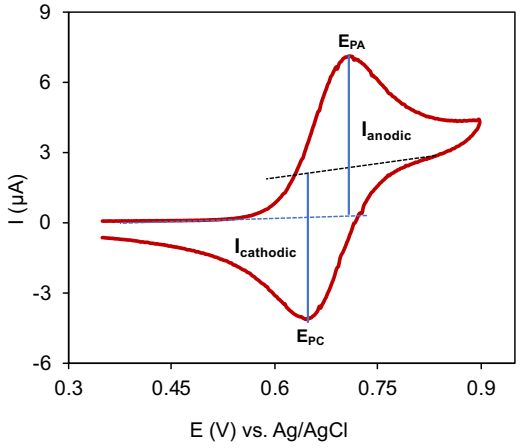

Figure 3. 1. Cyclic voltammogram of 1.0 mM TMB in $NaHCO_3$ (0.2 M). Scan rate: 25 mVs^{-1}.

By addition of 50 mM ethanol, the cyclic voltammogram of TMB displayed the characteristics of an oxidative EC′ reaction pathway, namely enhancement in the anodic peak current (nearly 3 times enhancement) and disappearance of the cathodic peak (**Figure 3.2**). The reduced form of TMB was oxidized to TMB^+ at the electrode surface and subsequently oxidized ethanol, generating acetaldehyde and the reduced form of TMB (TMBH). The consumption of TMB^+ by its chemical reaction with ethanol resulted in the observed cathodic peak disappearance, while the regeneration of TMBH during the chemical reaction and its oxidation at the electrode surface produced the current enhancement. The proposed mechanism is shown in Figure 3.2c. This mechanism has been proved in our previous studies.[31]

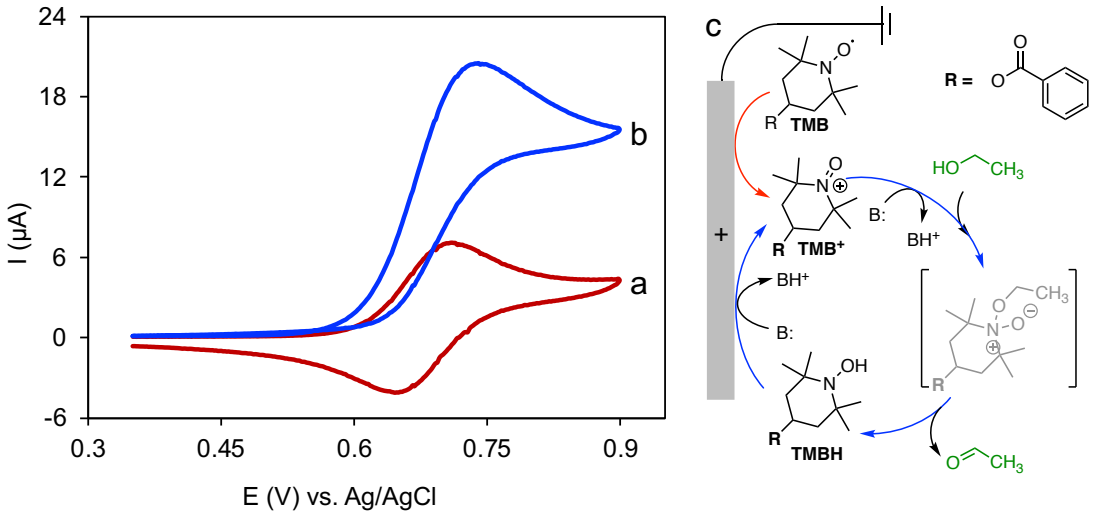

Figure 3. 2. Cyclic voltammograms of 1.0 mM TMB in $NaHCO_3$ (0.2 M) in the absence (a) and presence of 50 mM EtOH (b) and proposed catalytic cycle for the reaction (c). Scan rate: 25 mVs^{-1}.

As described in the introduction and demonstrated in Figure 3.2c, this catalytic reaction is strongly base-dependent; therefore, the effects of different bases were evaluated by voltammetric analysis. The catalytic activity of 1.0 mM TMB solution in the presence of excess

ethanol (50 mM) was examined under neutral and several basic aqueous conditions including NaCl, NaOAc, $NaHCO_3$, $NaHCO_3/Na_2CO_3$ buffer, and Na_2CO_3; the results are demonstrated in Figure 3.3. Under neutral conditions (NaCl), no catalytic activity was observed and the cyclic voltammogram was similar to that of TMB in the absence of ethanol. The catalytic activity increased as follows: NaOAc (45.5% enhancement) < $NaHCO_3$ (127% enhancement) < $NaHCO_3/Na_2CO_3$ buffer (762% enhancement) < Na_2CO_3 (1310% enhancement). This order corresponds to the order of basicity of the solutions.

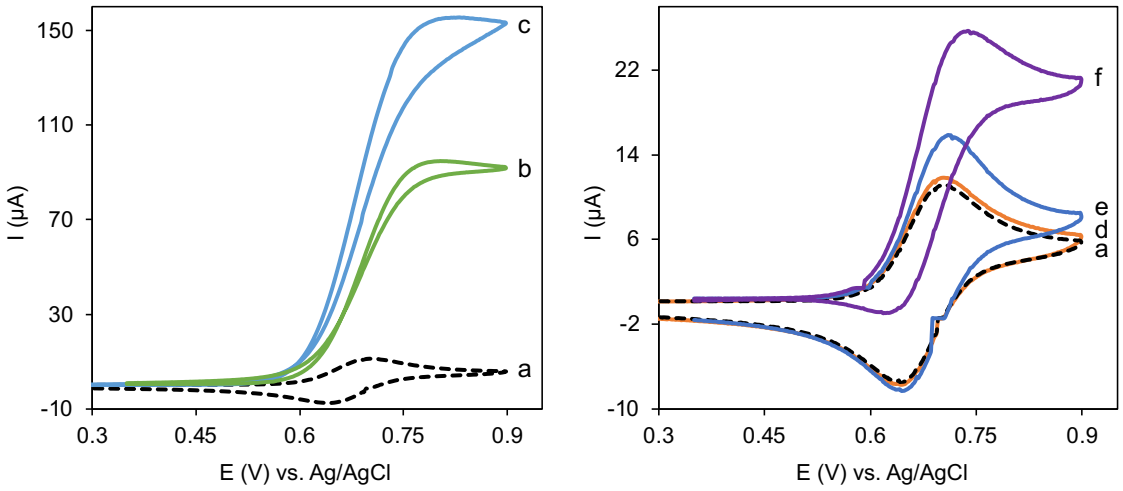

Figure 3. 3. Cyclic voltammograms of 1.0 mM TMB in the absence (a) and presence of 50 mM EtOH in $NaHCO_3/Na_2CO_3$ buffer (0.2 M) (b), Na_2CO_3 (0.2 M) (c), NaCl (0.2 M) (d), NaOAc (0.2 M) (e), $NaHCO_3$ (0.2 M) (f). Scan rate: 100 mVs^{-1}.

The redox reaction and catalytic activity of 2,2,6,6-tetramethylpiperidine *N*-oxyl (TEMPO) and 9-azabicyclo[3.3.1]nonane *N*-oxyl radical (ABNO) were also examined. TEMPO, as a representative aminoxyl compound, and ABNO, as a bicyclic aminoxyl with less steric hinderance as compared to TEMPO and TMB. TEMPO demonstrated similar reversibility as TMB, however significantly less catalytic activity toward ethanol oxidation.

This difference in reactivity can be attributed to the lower redox potential of TEMPO compared to TMB that makes $TEMPO^+$ a less potent oxidant. ABNO showed higher catalytic activity than TEMPO under mild basic conditions. Although ABNO has a similar redox potential to TEMPO, it has less steric hinderance which allows for more facile adduct formation between ethanol and its oxoammonium ($ABNO^+$), based on the proposed mechanism in Figure 3.2c. The catalytic activity of ABNO under mild basic conditions (pH ~9) is less than TMB, highlighting that redox potential has a greater effect on ethanol oxidation as compared to steric hinderance. Increasing basicity resulted in an irreversible electron transfer and less catalytic activity (lower oxidation current, **Figure 3.4**), unlike TMB. The lower steric hinderance of $ABNO^+$ makes it more susceptible to the formation of an electro-inactive adduct with hydroxide (OH^-) under more basic conditions.

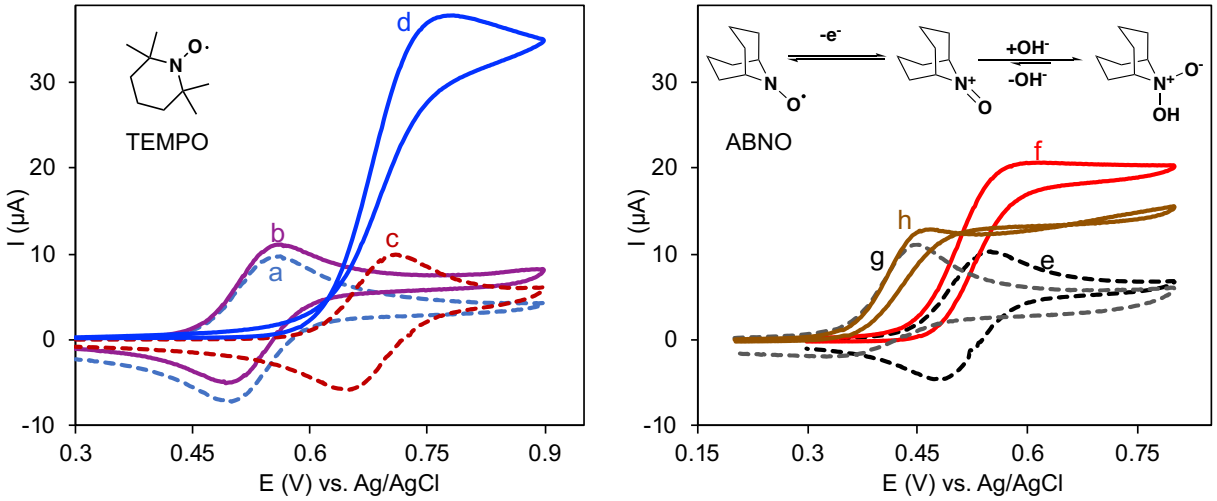

Figure 3. 4. Cyclic voltammograms of 1.0 mM TEMPO in the absence (a) and presence of 50 mM EtOH (b), 1.0 mM TMB in the absence (c) and presence of 50 mM EtOH (d), 1.0 mM ABNO in the absence (e) and presence of 50 mM EtOH (f) in $NaHCO_3$. Cyclic voltammogram of 1.0 mM ABNO in the absence (g) and presence of 50 mM EtOH (h) in Na_2CO_3. Scan rate: 50 mVs^{-1}.

3.2 Voltammetric Study of Ethanol Oxidation in Gas Phase: Fuel Cell Type Assembly

The initial electrochemical screening demonstrated efficient catalytic activity for the aminoxyl catalysts under mild basic conditions, and TMB with most catalytic activity. For solution based electrochemical reactions, the electrodes are connected by ionic conductivity of the dissolved supporting electrolyte that enables electrochemical measurements. To utilize this catalyst for ethanol oxidation in the breath, the reaction conditions need to be optimized for gas phase reactions. There are two possible options for electrochemical reaction in gas phase to achieve ion conductivity: utilizing either an ion-exchange membrane or a thin layer of a substance with ionic mobility between the working and counter electrodes. We attempted to fabricate a fuel cell type electrode using a Nafion membrane for ion-exchange. In this set up, the Nafion membrane would be modified with the aminoxyl catalyst on one side and a thin layer of polyaniline (PANI) on the opposite side to facilitate electron transfer; the modified membrane would be placed between two pieces of graphite which would be the working and counter electrodes (**Figure 3.5**).

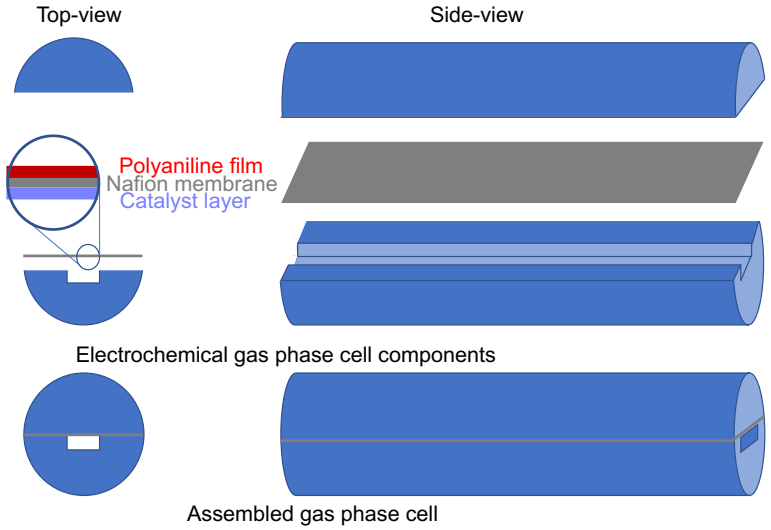

Figure 3. 5. Schematic presentation of the components and assembly of the fuel cell type electrodes.

To test the performance of each electrode reaction, PANI was electrochemically deposited onto the flat side of a half cylinder piece of graphite to make the electrode for the counter reaction. When the Nafion membrane was placed on top of the PANI-modified graphite, we still observed oxidation and reduction of the polymer via CV (**Figure 3.6**). Figure 3.6a shows the electrochemical oxidation of aniline and formation of PANI on the electrode surface, where A_1 corresponds to the oxidation peak of aniline and decreases in magnitude as the polymer is formed. A_2 and C_2 are the oxidation and reduction peaks, respectively, of the polymer and increase in magnitude as the polymer is formed. Figure 3.6b displays the cyclic voltammogram of PANI after deposition on the electrode surface in a supporting electrolyte solution without aniline, which proves the formation and redox activity of PANI under the experimental conditions.

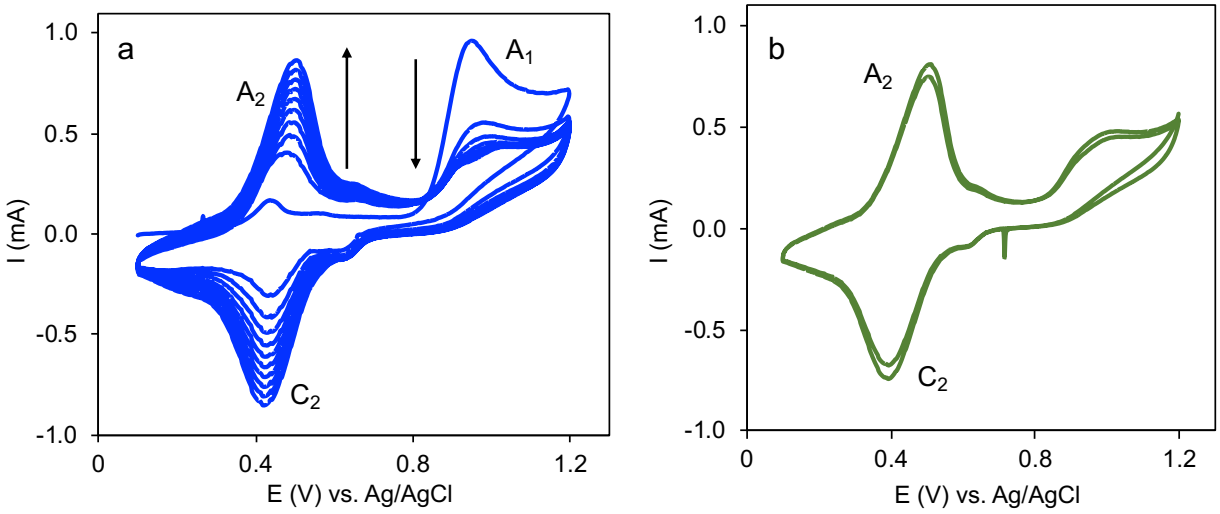

Figure 3. 6. Cyclic voltammograms of a 5.0 mM solution of aniline in 0.1 M H_2SO_4 supporting electrolyte (a) and the PANI-modified graphite electrode in only 0.1 M H_2SO_4 supporting electrolyte solution (b). Scan rate: 50 mVs^{-1}.

For fabrication of the working electrode, a Nafion based film with catalyst was deposited on a separate piece of graphite. Moving forward with TMB as our catalyst, we made an ink comprised of TMB, Nafion dispersion in water (as binder for the film), and graphene nanoplatelets (as conductive component of the film).[32,33] The catalyst ink was drop cast on a graphite electrode, allowed to dry and form a film (Nafion TMB film), and the electrode was subsequently placed in a mildly basic solution to test its electrochemical performance. The cyclic voltammogram showed redox features at the potentials similar to the redox features of TMB in solution, but with significantly higher background current and larger peak-to-peak separation, i.e., 210 mV (**Figure 3.7a**). We observed some improvement in these redox features by adjusting the composition of the film, for example the catalyst and graphene loading content.

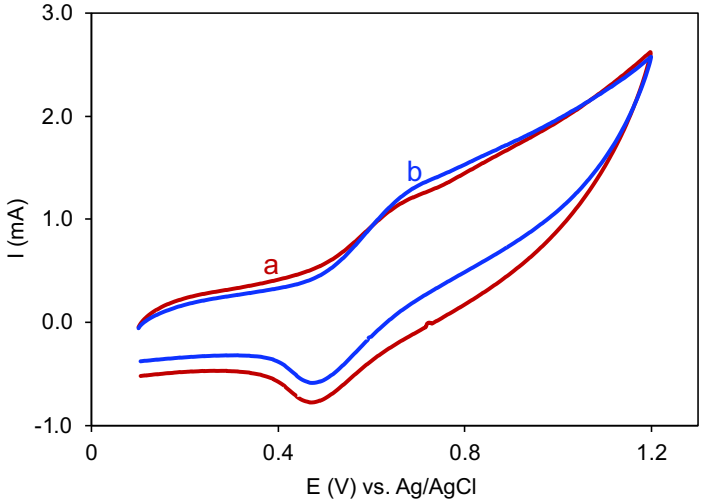

Figure 3. 7. Cyclic voltammograms of Nafion TMB film with Na_2CO_3 in the absence (a) and presence of 50 mM EtOH (b). The supporting electrolyte of the experiment was 0.2 M Na_2CO_3 or NaCl. Scan rate: 50 mVs^{-1}.

Upon addition of ethanol to the solution, the cyclic voltammogram of the modified graphite electrode did not show the expected signs of catalytic activity, including enhancement in oxidation current and disappearance of reduction peak (**Figure 3.7b**). We hypothesized that because of the nature of this proton-exchange membrane, basic anions do not diffuse into the structure of the film. Therefore, the required reaction components (base, catalyst, and ethanol) cannot interact as efficiently to facilitate the catalytic reaction. We had several attempts for changing the reaction conditions including changing base and its concentration, catalyst and its loading in the film, and incorporating the base into the ink and film, but no catalytic activity was observed in the presence of ethanol. Therefore, we moved on from the fuel cell idea and decided to attempt the other possible option of utilizing screen-printed electrodes.

3.3 Voltammetric Study of Ethanol Oxidation on Screen-Printed Electrode

Screen-printed electrode (SPE) is the assembly of the three electrodes needed for electrochemical studies printed or deposited at the surface of an insulating substance. The specific geometry of the SPE electrodes enables an electrochemical reaction in a small droplet where there is no need for the several-mL solution that is typically required for standard electrochemical cell (**Figure 3.8**).

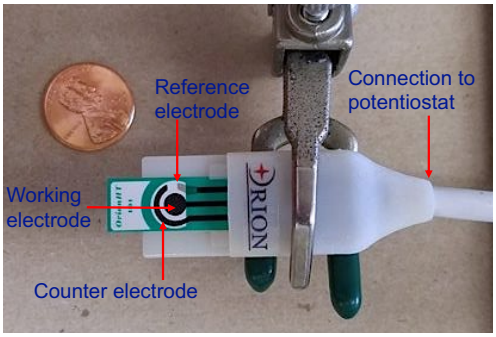

Figure 3. 8. A SPE with associated connection.

The droplet only needs to cover the surface of the electrode assembly in order to provide the ionic connectivity between them, making SPEs suitable for gas phase reactions. To examine the electrochemical performance of SPE, we used a droplet of solution with components similar to what has been used for the liquid phase studies.

Two solutions of 1.0 mM TMB in carbonate buffer were prepared, and to one of the solutions ethanol was added. A 10 µL droplet of each mixture was placed on the surface of two SPEs. The cyclic voltammogram of only TMB showed a smaller cathodic to anodic peak current ratio compared to Figure 3.1, indicating some side reaction of TMB^+ at the surface of the SPE (**Figure 3.9**). The change in shape and smaller peak current ratio of the cyclic voltammogram can be attributed to the interactions between TMB^+ and the components of the SPE carbon ink.

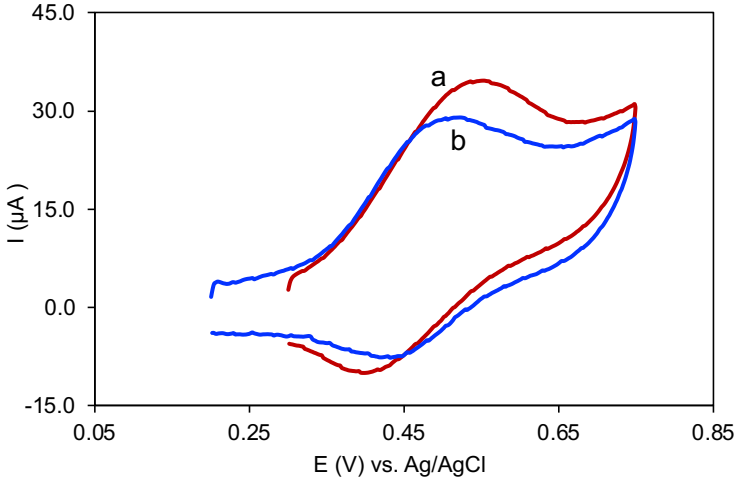

Figure 3. 9. Cyclic voltammograms of 1.0 mM TMB in the absence (a) and presence of 50 mM EtOH in $NaHCO_3/Na_2CO_3$ buffer, obtained using SPE. Scan rate: 100 mVs^{-1}.

More importantly, for the solution containing ethanol, no signs of catalytic activity were observed under these basic conditions. Under similar conditions, a seven-fold

enhancement in anodic peak current was observed for TMB using a glassy carbon electrode. To use SPEs for ethanol detection in gas phase, TEMPO, ABNO, and 4-acetamido-TEMPO (ACT) were also examined for their catalytic activity in these conditions. Voltammetric analysis of both TEMPO and ABNO showed even less reversibility than TMB; however, TEMPO showed some enhancement in anodic peak current in the presence of ethanol while ABNO showed no catalytic activity. ACT showed similar reversibility compared to TMB in the absence of ethanol but displayed a five-fold enhancement in anodic peak current on addition of ethanol (**Figure 3.10**). The redox potential of ACT and its catalytic activity in the liquid phase is similar to TMB. The significant catalytic activity of ACT compared to TMB at the surface of the SPE results from the structural differences between the two TEMPO derivatives, where ACT is much less hydrophobic and does not adsorb to the surface of the SPE like TMB.

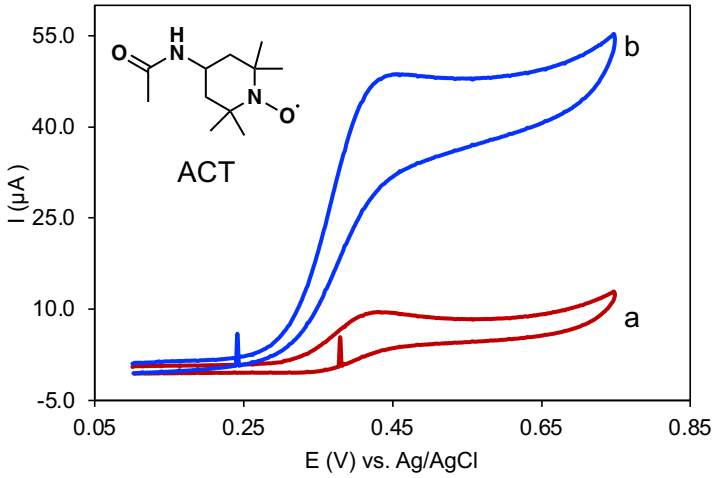

Figure 3. 10. Cyclic voltammograms of 1.0 mM ACT in the absence (a) and presence of 50 mM EtOH in $NaHCO_3/Na_2CO_3$ buffer, obtained using SPE. Scan rate: 100 mVs^{-1}.

Aqueous solutions are not ideal for ionic conductivity on SPEs. Less volatile and more viscous liquids would be ideal for this application and these characteristics can be found easily in ionic liquids. An ionic liquid (IL) is known as a salt that is liquid at room temperature (room temperature ionic liquid, or RTIL) or below 100°C, to extend the definition.[34] These substances are sometimes called liquid electrolytes and found several applications in electrochemistry as powerful solvents that can also be used as electrolytes.[35] Moreover, the cation or anion of the ionic liquid can be designed with acidic or basic characteristics for additional function in the reaction and elimination of some reaction components. One example is 1-ethyl-3-methylimidazolium acetate (EMIMAc), where the acetate gives it some basic characteristics and its low boiling point makes it a RTIL. To examine the catalytic behavior of TEMPO in this basic ionic media, a solution of TEMPO in MeCN was added to pure EMIMAc and a 10 µL droplet of the mixture was added to the surface of a carbon-based SPE. The cyclic voltammogram of TEMPO showed no reversibility in these conditions, indicated by the lack of a reduction peak (**Figure 3.11**).

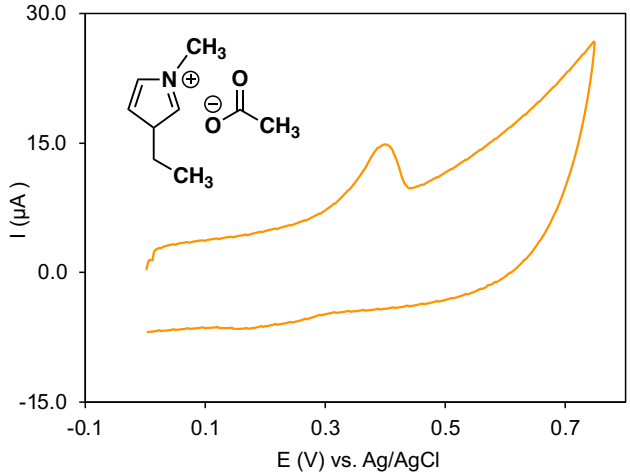

Figure 3. 11. Cyclic voltammogram of TEMPO in EMIMAc at the surface of the SPE. Scan rate: 50 mVs^{-1}.

We hypothesized that the high concentration of acetate anions in the IL had strong interaction with $TEMPO^+$, preventing its reduction. Therefore, we attempted to reduce the concentration of EMIMAc at the surface of the SPE by preparing a 1.2 M solution of the IL in water; however, upon addition of ethanol to the solution, no catalytic activity was observed. This proved that the interaction of $TEMPO^+$ and the acetate anions prevented ethanol oxidation by $TEMPO^+$. Moving to non-acetate ionic liquid and adding MeCN (nonpolar solvent) brought reversibility back, but no catalytic activity was observed.

We concluded that we should utilize a nonpolar binder instead and attempt to incorporate different bases; however, we will use ionic liquid to provide ionic connectivity between the electrodes on the SPE because of its high viscosity and nonvolatile characteristics. To achieve this, part of the working, counter, and reference electrodes will be covered with ionic liquid (please find the details in the experimental section). In our attempts for optimization of the reaction conditions for using ionic liquids, we noticed that the more hydrophobic character of MeCN, compared to water, enhanced the catalytic activity of the oxoammonium, as a charged species, toward ethanol oxidation. In other words, the order of reactivity of oxoammonium for ethanol oxidation is MeCN > water > ionic liquid. To test this hypothesis and take advantage of the enhanced catalytic activity in nonpolar conditions, we studied the possibility of using paraffin oil as a traditional binder for a carbon paste electrode (CPE). Fabrication of the carbon paste electrodes is described in detail in the experimental section.

3.4 Voltammetric Study of Ethanol Oxidation on Modified Carbon Paste Electrode

Composites of graphitic carbon with various active and inactive materials are commonly referred to as "carbon paste". Ralph N. Adams presented the first carbon paste electrode in 1958; now, traditional carbon paste electrodes are composed of graphite powder and a water-immiscible insulating organic liquid, often organic hydrocarbons such as Nafion or paraffin oil. The high volume fraction of graphite (typically > 50%) allows for contact between the particles and therefore a conducting pathway with suitably low bulk resistivity. Carbon pastes are particularly attractive for electrochemical applications because numerous kinds of reagents can be incorporated into the composition of the paste, like electrocatalysts, enzymes, and chemical recognition agents. To date, many carbon pastes have been synthesized that take advantage of this idea, producing carbon composite electrodes with unique reactivity or selectivity.[36,37] We have used this concept of CPE using paraffin oil as a nonpolar binder and different types of graphene. Based on the study of the reaction medium polarity described in section 3.3, the nonpolar character of paraffin should be promising for this catalytic reaction. We designed our first CPE based on graphene-to-binder ratios found in various literature sources,[38,39] finding that the ideal composition for our paste contained about 250 mg oil and 185 mg graphene nanoplatelets so that it held together and would adhere to the graphite electrode. The paste was pressed on the end of one graphite electrode with 5 mm diameter, one side shrouded in an insulating Teflon tube and the other side connected to potentiostat as demonstrated in **Figure 3.12**. Only the shrouded end with pressed CP was immersed in a solution of 1.0 mM ABNO under mild basic conditions that allowed electrochemical study of the paste.

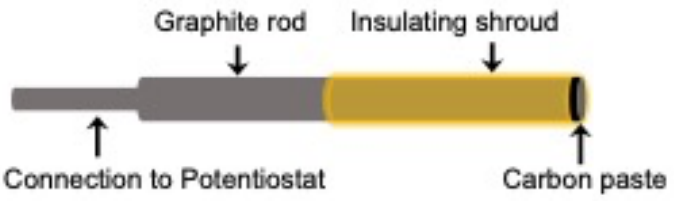

Figure 3. 12. Schematic structure of a graphite carbon paste electrode.

The cyclic voltammogram of ABNO showed a reversible signal, with a cathodic-to-anodic peak current ratio of unity and low background current under these conditions (**Figure 3.13**). High background current is observed for CPEs with inappropriate graphene-to-binder ratios. Thus, the ratio used for this study is suitable, indicating the effective conductivity of the paste. The peak current ratio of unity indicates the minimal interaction of oxoammonium with the components of this CPE, compared to the interactions observed at the surface of the SPEs.

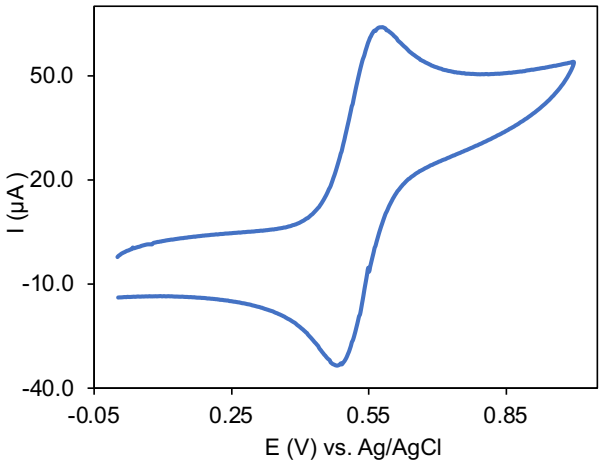

Figure 3. 13. Cyclic voltammogram of 1.0 mM ABNO in 0.2 M $NaHCO_3$ using CPE as working electrode. Scan rate: 100 mVs^{-1}.

Following the promising results, we attempted to incorporate our catalyst into the paste, examining the activity of both ABNO and TMB, named ABNOCPE and TMBCPE, respectively. The TMBCPE was placed into a solution of $NaHCO_3$ and the ABNOCPE was placed into a solution of KCl and lutidine. The initial cyclic voltammograms of both showed cathodic-to-anodic peak current ratios of unity and low background current (**Figure 3.14**, traces a and c).

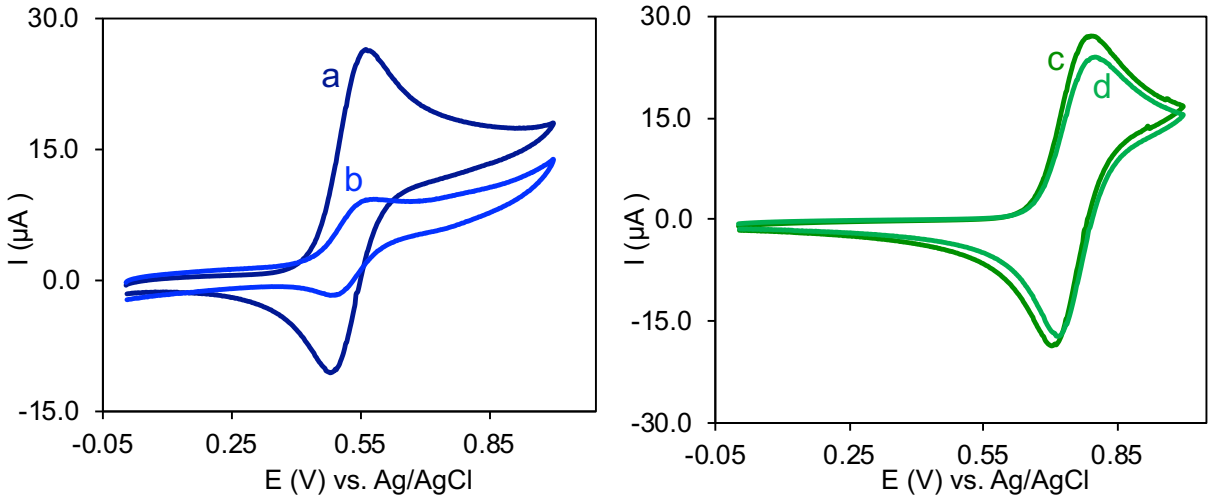

Figure 3. 14. Cyclic voltammograms of ABNOCPE in 0.2 M KCl and 0.2 M lutidine at t_0 (a) and t_{30} (b), and TMBCPE in 0.2 M $NaHCO_3$ at t_0 (c) and t_{30} (d). Scan rate: 25 mVs^{-1}.

After being in solution for 30 minutes, the cyclic voltammogram of TMBCPE did not show significant change; comparatively, the ABNOCPE current decayed substantially (approximately 3x). The decay can be attributed to the hydrophilic nature of ABNO, which caused it to leak from the paste over time, whereas the hydrophobic nature of TMB helped it stay within the paste.

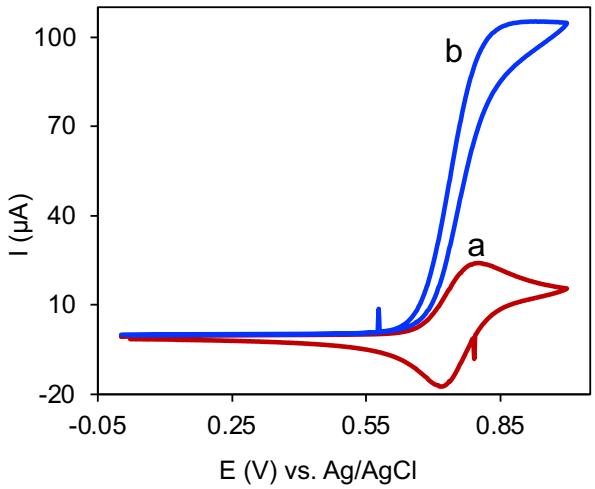

Figure 3. 15. Cyclic voltammograms of TMBCPE in 0.2 M $NaHCO_3$ in the absence (a) and presence of 50 mM EtOH (b). Scan rate: 25 mVs^{-1}.

Upon addition of ethanol to the solution after 30 minutes, ABNO and TMB displayed an enhancement in oxidation current, though TMB showed superior catalytic activity with four-fold enhancement in current (**Figure 3.15**) compared to the two-fold enhancement of ABNO (**Figure 3.17**, traces a and b), which agrees with the voltammetric results where the catalyst was in solution (**Figure 3.2** and **Figure 3.4**). Most importantly, the enhancement in catalytic current for TMBCPE is significantly higher than that of TMB in solution under the same basic conditions. This proves the effect of the nonpolar conditions of the paste on catalytic activity (CPE > MeCN > water > ionic liquid).

The catalytic activity of TMBCPE under mildly basic conditions prompted us to move forward and examine the effects of adding base to the carbon paste. Since $NaHCO_3$ was proven to be effective in facilitating the ethanol oxidation in solution, we added it into the paste. The carbon paste electrode modified with both TMB and $NaHCO_3$, called BTCPE was placed into

a KCl solution. TMBCPE has shown no catalytic activity in KCl, allowing for accurate evaluation of the effect of $NaHCO_3$ basicity on catalytic activity in the paste.

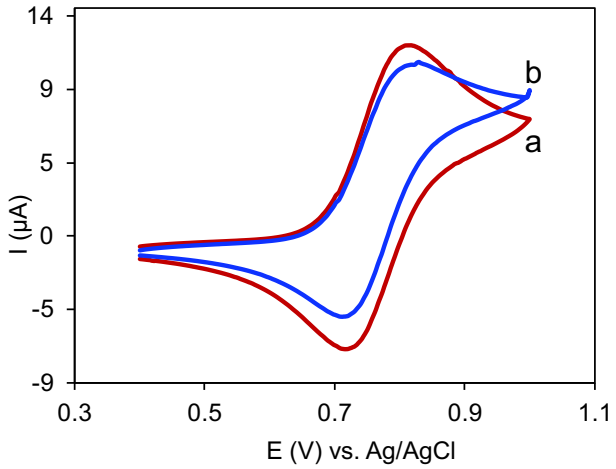

Figure 3. 16. Cyclic voltammograms of BTCPE in 0.2 M KCl in the absence (a) and presence of 50 mM EtOH (b). Scan rate: 25 mVs^{-1}.

BTCPE demonstrated a reversible signal corresponding to the redox reactions of TMB, similar to TMBCPE. Upon addition of ethanol, the cyclic voltammogram of BTCPE showed significantly diminished catalytic activity compared to TMBCPE (**Figure 3.16**). The lack of catalytic activity is related to the lack of interaction between TMB^+ and ethanol as a result of the insolubility of $NaHCO_3$ in the nonpolar carbon paste. Although it can be mixed into the paste, it is in a different phase than the hydrophobic TMB^+; in order for the base to facilitate the ethanol oxidation, all three components need to be able to come into contact. We concluded that a less polar organic base, soluble in paraffin oil and CPE matrix, would be necessary, and our first attempt was to use lutidine, a mildly basic organic compound. Since ABNO previously showed better catalytic activity in solution using lutidine as a base, we prepared a lutidine-

modified ABNOCPE (LACPE). The cyclic voltammogram of LACPE showed minimal enhancement of current and decrease in reduction peak current (**Figure 3.17**, traces c and d).

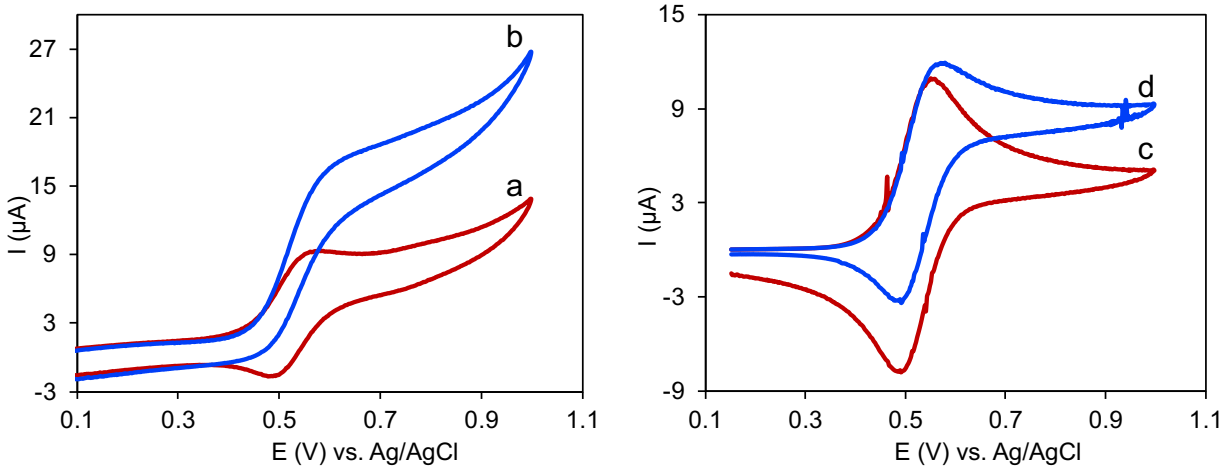

Figure 3. 17. Cyclic voltammograms of ABNOCPE in 0.2 M KCl and 0.2 M lutidine and LACPE in 0.2 M KCl in the absence (a, c, respectively) and presence of 50 mM EtOH (b, d, respectively). Scan rate: 25 mVs^{-1}.

The difference in catalytic activity using lutidine as a base, compared to carbonate buffer or Na_2CO_3, shows that lutidine is not basic enough to facilitate ethanol oxidation. In addition, the health and environmental hazards associated with lutidine present some challenges for practical use, prompting us to examine a structurally modified organic base, nicotinate, that has a basic carboxylate functional group. Moreover, nicotinate is the deprotonated form of nicotinic acid which is an essential nutrient with minimal environmental hazards. A solution of nicotinic acid (NA) in sodium hydroxide (NaOH) was prepared, generating the basic nicotinate ion; the TMBCPE was tested in this solution and the results are demonstrated in Figure 3.18.

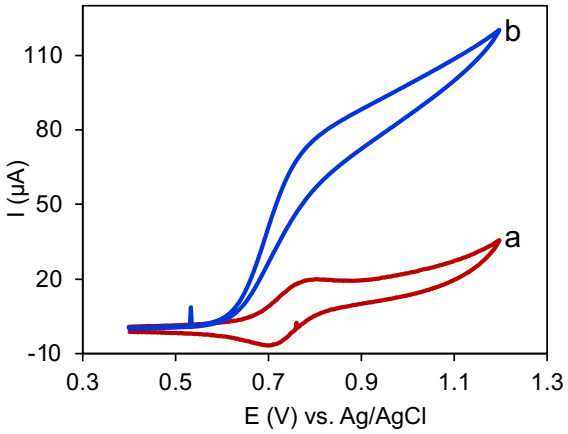

Figure 3. 18. Cyclic voltammograms of TMBCPE in 0.2 M NA/NaOH in the absence (a) and presence of 50 mM EtOH (b). Scan rate: 25 mVs^{-1}.

Upon addition of ethanol to the solution, a four-fold enhancement in current was observed (**Figure 3.18b**), comparable to the TMBCPE in a $NaHCO_3$ solution seen in Figure 3.16. ABNOCPE was also tested in the nicotinate solution; however, ABNO did not show reversibility. Because of the positive results with TMBCPE, we isolated the sodium nicotinate salt (NicH Nic^-) for incorporation into the paste. The cyclic voltammogram of this modified TMBCPE, NTCPE, displayed a slight enhancement in current with no decrease in reduction peak current. The observed results were similar to those of BTCPE.

3.5 Ethanol Oxidation on Paste Electrode with Basic Carbon

The significant difference of catalytic activity for paraffin-insoluble bases highlights the importance of a paste electrode with basic functional groups accessible to the catalyst in the paste and ethanol in gas phase. The best option to have accessible basic functional groups in the paste is using basic carbon materials. Carbon nanotubes and nanographene sheets are representative nanocarbon materials possessing distinctive mechanical, electrical, and

structural properties. They have been highlighted as useful materials for several important applications, including electronic devices, electromechanical devices, quantum wires, ultrahigh strength engineering fibers, and catalyst supports.[40] One possible way of expanding the applications of carbonaceous materials, especially the nanostructured materials, is to incorporate different functional groups into their structures. One of the functional groups that has been attached to the carbon structure is the carboxyl (COOH) group created by oxidation on nanocarbons.[41] The carboxylate-bearing carbon materials (including graphene) have shown different physical properties, like conductivity, compared to graphene itself. However, incorporation of the carboxylic acid or its conjugate form, carboxylate, gives acidic or basic character to the graphene oxides, respectively. Graphene oxide (GO) is 2D nanoplatelet that attracted recurring interest by the upsurge of graphene-related research in past two decades. The basic and acidic characters of these modified GO have been successfully utilized in numerous applications in electronics, conductive films, and composites.[42] These surface functionalities have shown significant improvement on properties of carbon materials for electrochemical applications that are highly surface sensitive. For the rest of this study, we had several attempts on utilization of the basic characteristic of GO to facilitate the aminoxyl-catalyzed ethanol oxidation without additional base. The catalytic performance of these GO electrodes and many of the above-mentioned electrodes was tested for ethanol oxidation in gas phase, where the counter electrode, reference electrode and part of the working electrode were covered by ionic liquid, to have the ionic conductivity. No significant catalytic activity was observed for ethanol oxidation in gas phase using electrodes described in section 3.4. The examples of CV study with no solvent using graphene and GO paste at SPE partially covered by 1-Butyl-3-methylimidazolium tetrafluoroborate ($BMIMBF_4$) are shown in Figure 3.19.

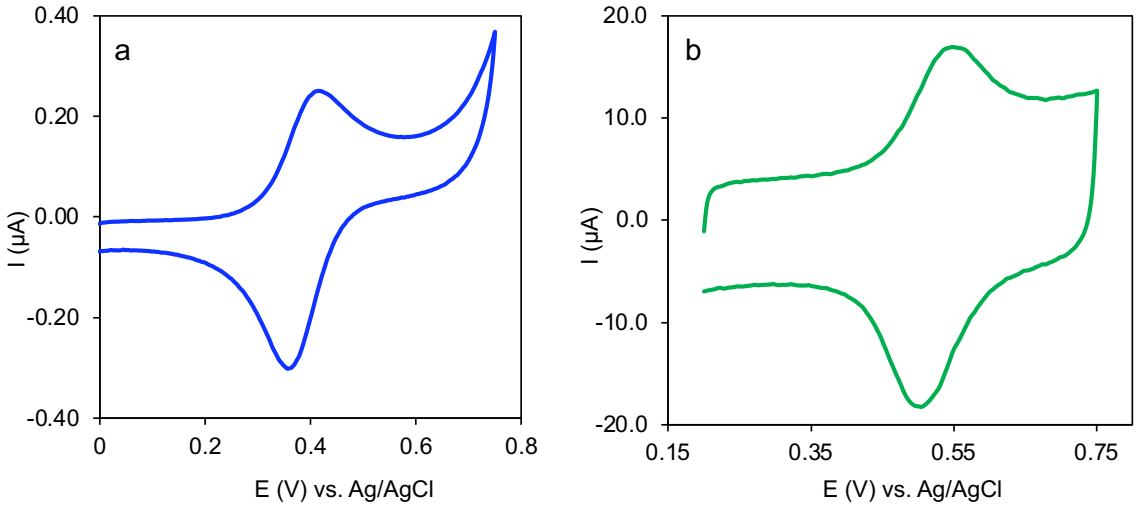

Figure 3. 19. Cyclic voltammograms of GACPE (a) and GOTCPE (b) at the surface of SPE. Reference and counter electrodes covered with $BMIMBF_4$. Scan rate: 25 mVs^{-1}.

The cyclic voltammogram of ABNO-modified graphene at the surface of SPE (GACPE) shows reversible redox features with anodic-to-cathodic peak current ratio of unity, similar to paste in aqueous solution that indicates ABNO molecules are accessible in the paste and the electrodes are connected in this electrode assembly (**Figure 3.19a**). The cyclic voltammogram of TMB-modified GO at the surface of SPE (GOTCPE) also displays reversible redox features at a higher potential corresponding to the higher redox potential of TMB compared to ABNO (**Figure 3.19b**). The anodic-to-cathodic peak current ratio of unity highlights the accessibility of TMB and stability of TMB^+ as well as the electrode connections via IL; however, the charging current for this paste is noticeably higher than that of GACPE. The charging current for CPE varies significantly by changing the composition of the paste, the particle size, and the surface area of the carbon materials, demonstrated in **Figure 3.20.**

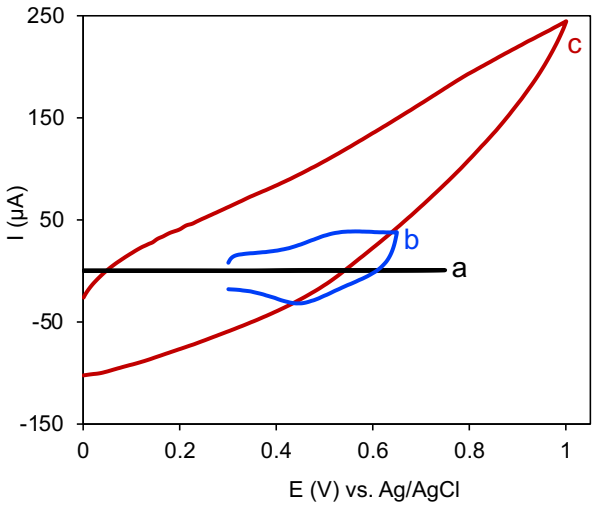

Figure 3. 20. Cyclic voltammograms of GACPE (a), NaOH-treated carbon paste (b), and chemically oxidized/NaOH-treated carbon paste (c) at the surface of SPE. Scan rate: 25 mVs^{-1}.

Graphene was treated with HNO_3, following a procedure reported in literature, to make GO.[43] The chemically oxidized graphene was then treated with NaOH in order to oxidize the carboxylic acid functional groups and generate the carboxylate within the structure of GO. For comparison, we also treated some graphene with NaOH, since there are some reports that graphene itself has some carboxylic acid functional groups. The basic graphene and GO particles were utilized to fabricate carbon pastes, with similar composition as the pastes made with commercially available GO and graphene (shown in Figure 3.20). Figure 3.20 demonstrates the difference in the charging currents of the graphene and these two modified carbon pastes. When graphene was treated only with NaOH (**Figure 3.20b**), the resulting charging current was significantly higher than that observed with GACPE (**Figure 3.20a**). When graphene was chemically oxidized and then treated with NaOH (**Figure 3.20c**), the increase in charging current was substantially higher. When the cyclic voltammograms are overlayed using the same scale, the difference is so prominent that the signal for GACPE

becomes a horizontal line. These results prove the change in background current for different carbon materials and show that any extra step will cause an increase in the charging current. We have also noticed that some of the fine particles of GO pass through the filter and, consequently, the morphology of the resulted carbon after the chemical treatments is not the same as the initial form of graphene or GO. Based on these changes and appearance of unwanted charging current after each step, we decided to use commercially available GO and minimize chemical treatment and filtration. With the reported loading of carboxylic acid functional groups of GO stated on the supplier website, we calculated the amount of NaOH required for turning the carboxylic acid functional groups to carboxylate in GO (see Experimental section). The mixture was kept under vacuum to evaporate the water that was added with NaOH, and the resulting basic GO (BGO) was used, with no filtration, to make the pastes (**Figure 3.21**).

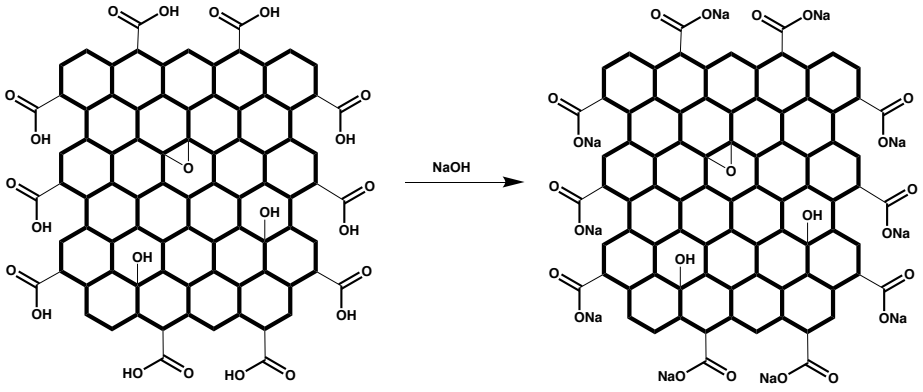

Figure 3. 21. Schematic presentation of graphene oxide structure and its deprotonation by NaOH.

The isolated BGO was ground to ensure the particles were small and a paste was made by mixing this BGO with TMB and paraffin oil. TMB was utilized as the most efficient catalyst for this ethanol oxidation. The paste was deposited onto the surface of a SPE, and the reference

and counter electrodes were covered with 1 M KCl. Because of the low viscosity of the ionic liquid and its wetting properties for covering the electrode body that is made of plastic, we had some issues in making the three electrodes connected with this specific ionic liquid. Using aqueous KCl solution instead helped us to resolve the issue, but further optimization of the ionic liquid is required since the nonvolatile character of ionic liquid is needed for shelf-life stability of the electrodes. The fabricated electrode (BGOCPE) gave a cyclic voltammogram with high charging current and existing, though ill-defined, redox features (**Figure 3.22a**). The redox features correspond to oxidation of TMB (A_1) and reduction of TMB^+ (C_1).

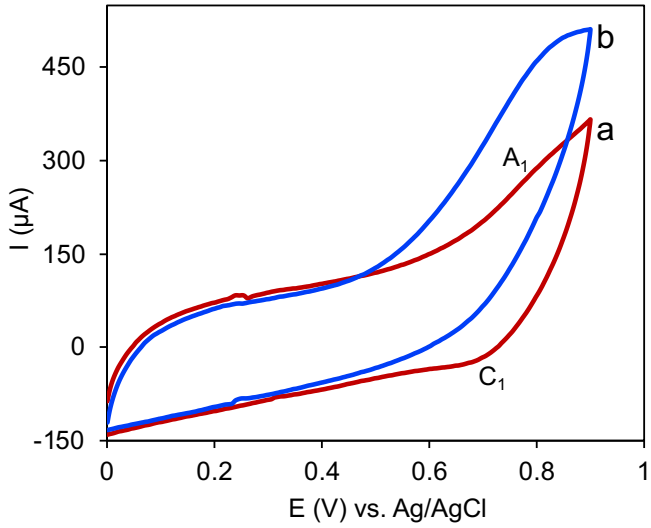

Figure 3. 22. Cyclic voltammograms of BGOCPE in the absence (a) and presence of 135 mM EtOH vapor (b). Reference and counter electrodes covered with 1 M KCl. Scan rate: 25 mVs^{-1}.

By exposing this electrode to a gas flow with ethanol content similar to the breath that corresponds to 0.08 BAC, the features of catalytic reactions appeared on the cyclic voltammogram of BGOCPE (**Figure 3.22b**). The current enhancement as a result of catalytic activity proves the contribution of basic GO on ethanol oxidation. To avoid the high charging

current for this modified GO (compared to graphene itself with negligible charging current), different mixtures of BGO and graphene were used for fabrication of CPEs. The 50:50 mixture of graphene and BGO (GGOCPE) resulted in cyclic voltammograms with ten-fold smaller charging current and more well-defined redox features, where the electrode showed the same catalytic performance (**Figure 3.23**).

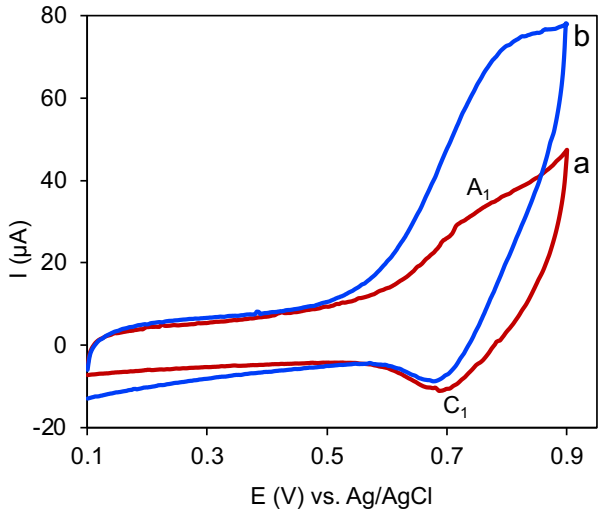

Figure 3. 23. Cyclic voltammograms of GGOCPE in the absence (a) and presence of 135 mM EtOH vapor (b). Reference and counter electrodes covered with 1 M KCl. Scan rate: 25 mVs^{-1}.

To simplify the electrochemical process, a chronoamperometric technique was used in which sufficiently high potential for TMB/TMB^{+} oxidation was applied (i.e., 0.9 V) and the current enhancement as the result of TMB^{+} catalyzed oxidation of ethanol was monitored over time (i.e., 20 seconds). In the absence of ethanol, the resulting chronoamperograms for BGOCPE and GGOCPE show an initial current corresponding to the oxidation of TMB molecules, and the current decays over time as all the TMB is oxidized (**Figure 3.24**, trace a and d, respectively).

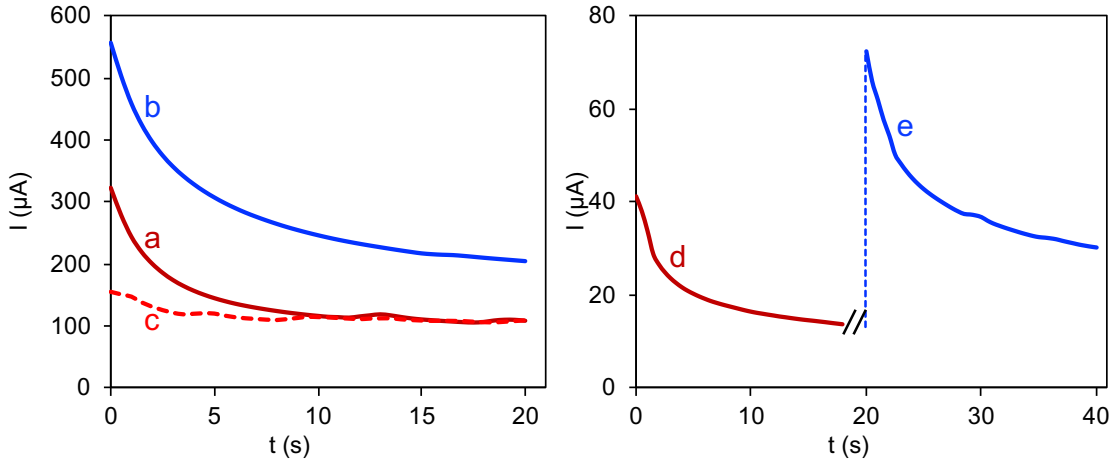

Figure 3. 24. Chronoamperograms of BGOCPE in the absence (a – initial, and c – after EtOH exposure) and presence of 135 mM EtOH in gas phase (b), and GGOCPE in the absence (d) and presence of 135 mM EtOH in gas phase (e). Applied potential: 1 V.

In the presence of ethanol, the initial current observed is significantly higher due to the turnover of TMB as it is oxidized and then oxidizes ethanol, regenerating TMBH to undergo another catalytic cycle (**Figure 3.24**, trace b and e, respectively). Thus, BGOCPE and GGOCPE display catalytic activity in the presence of ethanol as indicated by the increased current upon exposure to ethanol-containing vapors. The difference in charging current that was seen on the cyclic voltammograms can also be seen on the chronoamperograms, as the current in the absence of ethanol is eight-fold higher for BGOCPE than for GGOCPE. After exposure to ethanol, the BGOCPE was again exposed to only water vapor and the current returned to a similar value as was observed before exposure to ethanol (**Figure 3.24c**).

3.6 Ethanol Oxidation on Basic Graphene Oxide Screen-Printed Electrodes

The results of this basic GO are promising for further application, but the interest in exploring the properties of GO in electrochemistry made GO-based SPEs commercially available recently. With similar concept as BGOCPE, GO-based SPEs (GOSPEs) were obtained and treated with various amounts of NaOH in order to generate the basic carboxylate groups at the surface of the SPE. This eliminates the need for modification of a carbon-based SPE with GO and makes the process of electrode fabrication easier. A catalyst solution containing TMB and paraffin oil was drop cast on the surface of the basic GOSPE (BGOSPE). The resulted BGOSPE with TMB should have similar composition as BGOCPE, including catalyst, BGO, and paraffin. To find the appropriate amount of base required for deprotonation of the carboxylic acid groups, the electrode surface (just working electrode area) was covered with 10 uL aqueous solutions with different NaOH concentrations. The electrode was left to dry and then modified with TMB and paraffin oil (see experimental section). Figure 3.25 shows the redox features and catalytic performance of these electrodes for ethanol oxidation.

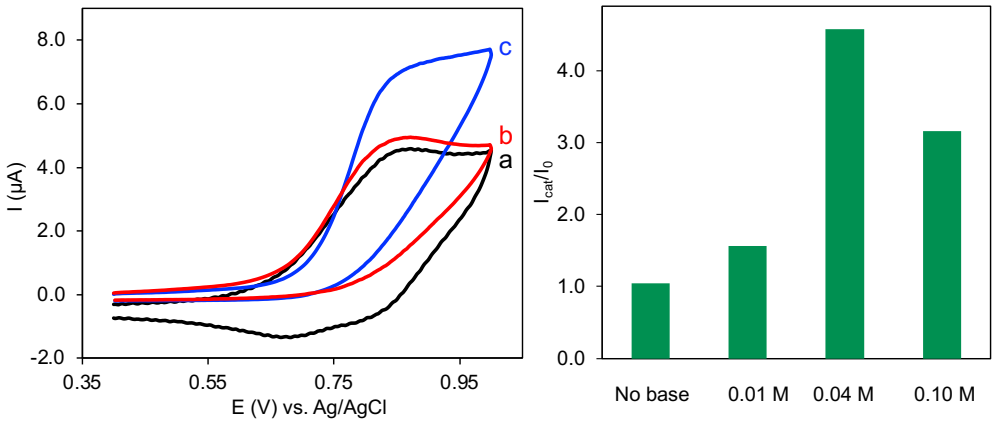

Figure 3. 25. Left: cyclic voltammograms of untreated GOSPE (a) and BGOSPE treated with 0.01 M NaOH in the absence (b) and presence of 135 mM EtOH vapor (c). Scan rate: 25 mV s^{-1}. Right: I_{cat}/I_0 for BGOSPEs treated with various amounts of NaOH.

The cyclic voltammogram of the untreated GOSPE shows an oxidation peak, similar to GOTCPE, but the reduction peak was ill-defined on the reverse scan (**Figure 3.25a**). This can likely be attributed to interaction by TMB with some component of the ink used to fabricate the GOSPE. The BGOSPE treated with 0.01 M NaOH gave a cyclic voltammogram with no reduction peak, in the absence of ethanol, indicating more side reactions for TMB under this basic condition (**Figure 3.25b**). However, a reasonable enhancement in current was observed upon exposure to ethanol vapors, indicating that TMB could effectively oxidize ethanol (**Figure 3.25c**). All of the BGOSPEs displayed an enhancement in current upon exposure to ethanol vapors, signifying that the electrodes were basic enough to facilitate ethanol oxidation. To compare the BGOSPE performances, the ratio of catalytic peak current (in the presence of ethanol, I_{cat}) to anodic peak current (in the absence of ethanol, I_0) was plotted against the NaOH concentrations; this showed that the BGOSPE treated with 0.04 M NaOH provided the most substantial catalytic response (**Figure 3.25**, right). After optimization of the base, the catalyst concentration was also optimized. Figure 3.26 shows I_0, I_{cat}, and their ratios, for different concentrations of TMB.

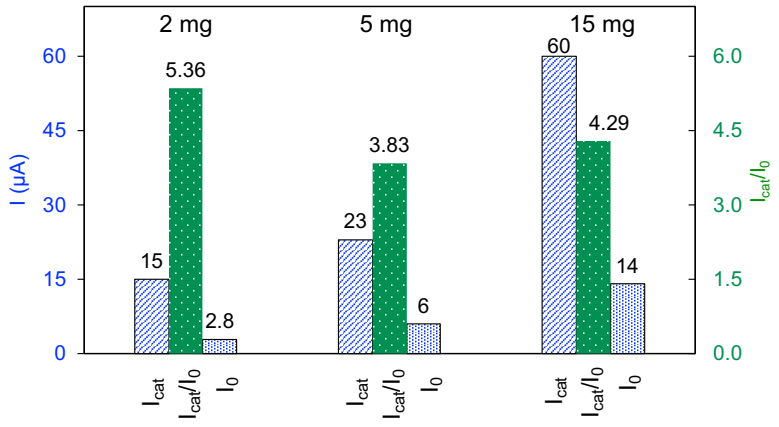

Figure 3. 26. I_0, I_{cat}, and their ratios for oxidation current for BGOSPE with different TMB loading.

Increasing the catalyst concentration caused enhancement in both I_0 and I_{cat} intensity, but the modified electrode with the solution bearing 2 mg of TMB resulted in the highest ratio and most catalytic activity. This electrode was used further to examine the correlation of catalytic current and ethanol concentration in the gas phase. It should be noted that catalyst loading was also optimized for BGOCPE, and similar trends were observed with less reproducibility.

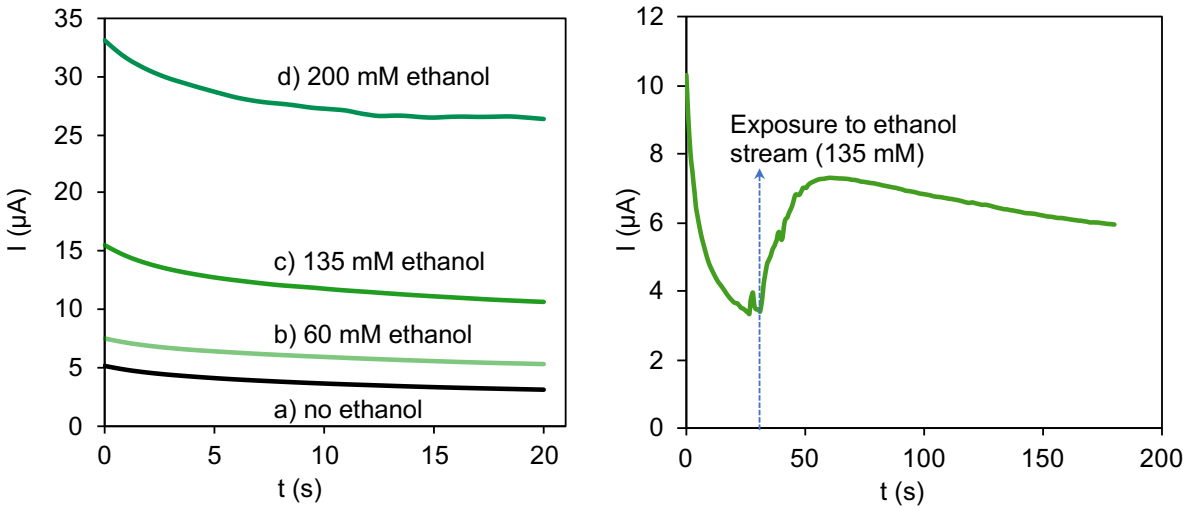

Figure 3. 27. Left: Chronoamperograms of GOSPE in the absence and presence of different concentrations of EtOH vapor; right: response time of GOSPE toward EtOH vapor. Applied potential: 1 V.

Figure 3.27 (left) demonstrates the sensitivity of BGOSPE toward varying concentrations of ethanol vapors. As BGOSPE was exposed to increasing amounts of ethanol, the chronoamperograms displayed higher current with the same applied potential over time due to the increased number of catalytic cycles as TMB oxidized more ethanol. The ethanol concentrations for the solutions which the gas passed through to simulate breath were 60 mM, 135 mM, and 200 mM; these concentrations give BrAC values corresponding to 0.035%,

0.08%, and 0.118% BAC, respectively. The response time of BGOSPE toward ethanol vapor was also examined (**Figure 3.27**, right). The electrode was first exposed to water vapor for about 20 seconds while sufficient potential was applied for oxidation of TMB/TMB^+ (i.e., 1.0 V) and the expected decay in current was observed as TMB was consumed. Upon exposure to the ethanol stream, the current began to increase as ethanol was oxidized and catalytic turnovers were achieved. The current reached its maximum value after about 20 seconds.

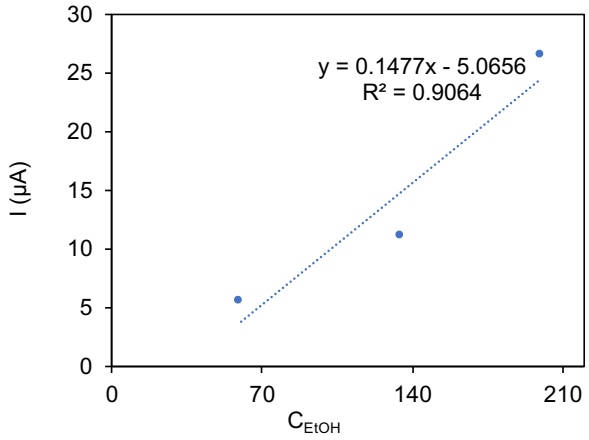

Figure 3. 28. Correlation of I_{cat} and EtOH concentration for BGOSPE.

The BGOSPEs showed an increasing value of I_{cat} as the concentration of ethanol was increased (**Figure 3.28**), which proved that the electrodes were sensitive to different amounts of ethanol. However, the trend is not perfectly linear, indicating that further optimization is needed for these electrodes.

CONCLUSION AND OUTLOOK

The results described in this thesis show the successful utilization of the unique catalytic activity of the aminoxyl radical/oxoammonium redox couple toward alcohol oxidation for fabrication of an electrochemical ethanol sensor for breath analysis. Our functional sensing element consists of a screen-printed electrode in which the graphene oxide-based working electrode is modified with aminoxyl derivatives. Exposing this modified electrode to simulated breath that contains ethanol, while applying the required potential for oxidation of aminoxyl radical, generates an electrocatalytic current proportional to the ethanol concentration in the breath. Though we found 4-hydroxy-2,2,6,6-tetramethylpiperidine 1-oxyl benzoate (TMB) to be the most efficient aminoxyl in our studies, the wide variety of aminoxyl derivatives that exist allow for deeper studies of our foundational work.

With this proof-of-concept work, careful optimization is necessary for high reproducibility and commercial use. For example, optimization for different breath size/flow rate is crucial. Additionally, designing the electrode shape and sensing element sizes are key points. One possible design is a cone shaped electrode in which the smaller opening is the outlet that limits the flow rate and provides a reasonable residence time for the ethanol vapor. Signal recording is limited by the length of time that potential is applied; the readout for the user is the charge consumed or current per certain amount of time. After the sensing element is optimized, it can be coupled with a simple, miniaturized potentiostat or power supply that reads the current as the result of an applied, fixed potential. The potential is determined based on the nature of catalyst under the reaction conditions. These simple, sensitive, durable, and inexpensive electrodes may contribute to the development of a single-use reliable ethanol sensor for personal or law enforcement applications.

REFERENCES

1. National Institute on Alcohol Abuse and Alcoholism. *Alcohol Facts and Statistics*; 2017.

2. National Highway Traffic Safety Administration; US Department of Transportation. *2016 Data: Alcohol-Impaired Driving*; 2016.

3. Dombrink, K. J. A Commercial Device Involving the Breathalyzer Test Reaction. *J. Chem. Educ.* **1996**, *73*, 135.

4. Jones, A.; Andersson, L. Variability of the Blood/Breath Alcohol Ratio in Drinking Drivers. *J. Forensic Sci.* **1996**, *41*, 916.

5. Skoog, D. A.; Holler, F. J.; Crouch, S. R. Gas Chromatography. In *Principles of Instrumental Analysis*; Cengage Learning, 2018; pp 720–740.

6. van Fleet, T. R.; Philip, B. K. Acetaldehyde. *Encyclopedia of Toxicology*; Wexler, P., Ed.; Academic Press, 2014; pp 22–23.

7. Matsumura, Y.; Stiles, K. M.; Reid, J.; Frenk, E. Z.; Cronin, S.; Pagovich, O. E.; Crystal, R. G. Gene Therapy Correction of Aldehyde Dehydrogenase 2 Deficiency. *Mol. Ther. Methods Clin. Dev.* **2019**, *15*, 72.

8. Yang, S.-J.; Wang, H.-Y.; Li, X.-Q.; Du, H.-Z.; Zheng, C.-J.; Chen, H.-G.; Mu, X.-Y.; Yang, C.-X. Genetic Polymorphisms of ADH2 and ALDH2 Association with Esophageal Cancer Risk in Southwest China. *World J. Gastroenterol.* **2007**, *13*, 5760.

9. Morey, T. E.; Booth, M. M.; Prather, R. A.; Nixon, S. J.; Boissoneault, J.; Melker, R. J.; Goldberger, B. A.; Wohltjen, H.; Dennis, D. M. Measurement of Ethanol in Gaseous Breath Using a Miniature Gas Chromatograph. *J. Anal. Toxicol.* **2011**, *35*, 134.

10. Xu, M.; Tang, Z.; Duan, Y.; Liu, Y. GC-Based Techniques for Breath Analysis: Current Status, Challenges, and Prospects. *Crit. Rev. Anal. Chem.* **2016**, *46*, 291.

11. Cremer, E.; Gruber, H. L.; Huck, H. Electro-Chemical Detector for Gas Chromatographic Determination of Alcohols and Aldehydes. *Chromatographia* **1969**, *2*, 197.

12. Allan, J. T. S.; Rahman, M. R.; Easton, E. B. The Influence of Relative Humidity on the Performance of Fuel Cell Catalyst Layers in Ethanol Sensors. *Sens. Actuators, B* **2017**, *239*, 120.

13. Gamella, M.; Campuzano, S.; Manso, J.; Gonzalez de Rivera, G.; Lopez-Colino, F.; Reviejo, A. J.; Pingarron, J. M. A Novel Non-Invasive Electrochemical Biosensing Device for in Situ Determination of the Alcohol Content in Blood by Monitoring Ethanol in Sweat. *Anal. Chim. Acta* **2014**, *806*, 1.

14. Kim, J.; Jeerapan, I.; Imani, S.; Cho, T. N.; Bandodkar, A.; Cinti, S.; Mercier, P. P.; Wang, J. Noninvasive Alcohol Monitoring Using a Wearable Tattoo-Based Iontophoretic-Biosensing System. *ACS Sens.* **2016**, *1*, 1011.

15. Bihar, E.; Deng, Y.; Miyake, T.; Saadaoui, M.; Malliaras, G. G.; Rolandi, M. A Disposable Paper Breathalyzer with an Alcohol Sensing Organic Electrochemical Transistor. *Sci. Rep.* **2016**, *6*, 27582.

16. Nutting, J. E.; Rafiee, M.; Stahl, S. S. Tetramethylpiperidine N-Oxyl (TEMPO), Phthalimide N-Oxyl (PINO), and Related N-Oxyl Species: Electrochemical Properties and Their Use in Electrocatalytic Reactions. *Chem. Rev.* **2018**, *118*, 4834.

17. Golubev, V. A.; Rozantsev, E. G.; Neiman, M. B. Some Reactions of Free Iminoxyl Radicals with the Participation of the Unpaired Electron. *Bull. Acad. Sci. USSR, Chem. Ser.* **1965**, *14*, 1898.

18. Iwabuchi, Y. Discovery and Exploitation of AZADO: The Highly Active Catalyst for Alcohol Oxidation. *Chem. Pharm. Bull.* **2013**, *61*, 1197.

19. Rafiee, M.; Konz, Z. M.; Graaf, M. D.; Koolman, H. F.; Stahl, S. S. Electrochemical Oxidation of Alcohols and Aldehydes to Carboxylic Acids Catalyzed by 4-Acetamido-TEMPO: An Alternative to "Anelli" and "Pinnick" Oxidations. *ACS Catal.* **2018**, *8*, 6738.

20. Rafiee, M.; Alherech, M.; Karlen, S. D.; Stahl, S. S. Electrochemical Aminoxyl-Mediated Oxidation of Primary Alcohols in Lignin to Carboxylic Acids: Polymer Modification and Depolymerization. *J. Am. Chem. Soc.* **2019**, *141*, 15266.

21. Semmelhack, M. F.; Chou, C. S.; Cortes, D. A. Nitroxyl-Mediated Electrooxidation of Alcohols to Aldehydes and Ketones. *J. Am. Chem. Soc.* **1983**, *105*, 4492.

22. Yamauchi, Y.; Maeda, H.; Ohmori, H. Amperometric Detection of Alcohols and Carbohydrates Coupled with Their Electrocatalytic Oxidation by 2,2,6,6-Tetramethylpiperidinyl-1-Oxy (TEMPO). *Chem. Pharm. Bull.* **1996**, *44*, 1021.

23. Rafiee, M.; Miles, K. C.; Stahl, S. S. Electrocatalytic Alcohol Oxidation with TEMPO and Bicyclic Nitroxyl Derivatives: Driving Force Trumps Steric Effects. *J. Am. Chem. Soc.* **2015**, *137*, 14751.

24. Hickey, D. P.; Schiedler, D. A.; Matanovic, I.; Doan, P. V.; Atanassov, P.; Minteer, S. D.; Sigman, M. S. Predicting Electrocatalytic Properties: Modeling Structure-Activity Relationships of Nitroxyl Radicals. *J. Am. Chem. Soc.* **2015**, *137*, 16179.

25. Hoover, J. M.; Steves, J. E.; Stahl, S. S. Copper(I)/Tempo-Catalyzed Aerobic Oxidation of Primary Alcohols to Aldehydes with Ambient Air. *Nat. Protoc.* **2012**, *7*, 1161.

26. Huang, Y.; Ren, J.; Qu, X. Nanozymes: Classification, Catalytic Mechanisms, Activity Regulation, and Applications. *Chem. Rev.* **2019**, *119*, 4357.

27. Kashiwagi, Y.; Ono, T.; Sato, F.; Kumano, M.; Yoshida, K.; Dairaku, T.; Sasano, Y.; Iwabuchi, Y.; Sato, K. Electrochemical Determination of Choline Using Nortropine-N-Oxyl for a Non-Enzymatic System. *Sens. Bio-Sens. Res.* **2020**, *27*, 100302.

28. Kashiwagi, Y.; Uchiyama, K.; Kurashima, F.; Kikuchi, C.; Anzai, J. Chiral Discrimination in Electrocatalytic Oxidation of (R)- and (S)-1-Penylethanol Using a Chiral Nitroxyl Radical as Catalyst. *Chem. Pharm. Bull.* **1999**, *47*, 1051.

29. Screen-Printed Electrodes. https://www.dropsens.com/en/screen_printed_electrodes_pag.html (accessed 2021 -10 -24).

30. Pratzler, S.; Knopf, D.; Ulbig, P.; Scholl, S. Preparation of Calibration Gas Mixtures for the Measurement of Breath Alcohol Concentration. *J. Breath Res.* **2010**, *4*, 036004.

31. Goes, S. L.; Mayer, M. N.; Nutting, J. E.; Hoober-Burkhardt, L. E.; Stahl, S. S.; Rafiee, M. Deriving the Turnover Frequency of Aminoxyl-Catalyzed Alcohol Oxidation by Chronoamperometry: An Introduction to Organic Electrocatalysis. *J. Chem. Educ.* **2021**, *98*, 600.

32. Ungan, H.; Bayrakçeken Yurtcan, A. PEMFC Catalyst Layer Modification with the Addition of Different Amounts of PDMS Polymer in Order to Improve Water Management. *Int. J. Energy Res.* **2019**, *43*, 5946.

33. Sarikaya, S.; Ozcan, M.; Uzunoglu, A. Modification of Commercial Pt/C Catalyst with Graphene Nanoplatelets for Sensitive and Selective Detection of Acetaminophen in Commercial Tablets. *ECS J. Solid State Sci. Technol.* **2020**, *9*, 115006.

34. Ionic Liquid. https://en.wikipedia.org/wiki/Ionic_liquid (accessed 2021 -11 -02).

35. Armand, M.; Endres, F.; MacFarlane, D. R.; Ohno, H.; Scrosati, B. Ionic-Liquid Materials for the Electrochemical Challenges of the Future. *Nat. Mater.* **2009**, *8*, 621.

36. Kalcher, K. Chemically Modified Carbon Paste Electrodes in Voltammetric Analysis. *Electroanalysis* **1990**, *2*, 419.

37. McCreery, R. L. Advanced Carbon Electrode Materials for Molecular Electrochemistry. *Chem. Rev.* **2008**, *108*, 2646.

38. Kamyabi, M. A.; Aghajanloo, F. Electrocatalytic Oxidation and Determination of Nitrite on Carbon Paste Electrode Modified with Oxovanadium(IV)-4-Methyl Salophen. *J. Electroanal. Chem.* **2008**, *614*, 157.

39. Zare, H. R.; Nasirizadeh, N.; Mazloum Ardakani, M. Electrochemical Properties of a Tetrabromo-p-Benzoquinone Modified Carbon Paste Electrode. Application to the Simultaneous Determination of Ascorbic Acid, Dopamine and Uric Acid. *J. Electroanal. Chem.* **2005**, *577*, 25.

40. Shu, Y.; You, T.; Liang, B.; Chen, H.; Yin, P. Bioinspired Ternary Artificial Nacre Graphene Oxide/Carboxyl Functionalized Single-Walled Carbon Nanotubes/Konjac Glucomannan with Enhanced Mechanical Properties. *ACS Appl. Bio Mater.* **2019**, *2*, 5544.

41. Stein, A.; Wang, Z.; Fierke, M. A. Functionalization of Porous Carbon Materials with Designed Pore Architecture. *Adv. Mater.* **2009**, *21*, 265.

42. Dimiev, A. M.; Tour, J. M. Mechanism of Graphene Oxide Formation. *ACS Nano* **2014**, *8*, 3060.

43. Jansen, R. J. J.; van Bekkum, H. XPS Of Nitrogen-Containing Functional Groups On Activated Carbon. *Carbon* **1995**, *33*, 1021.

VITA

Mikayla Mayer was born in Lodi, California on the 14th of November 1997, and moved to St. Charles, Missouri when she was three years old. Following her graduation from Timberland High School in Wentzville, Missouri, she attended University of Missouri-Kansas City for undergraduate studies. In the spring of 2020, she joined Prof. Rafiee's research group. That semester, she graduated with her B.S. in Chemistry. She began her masters studies that same year at University of Missouri-Kansas City under the guidance of Prof. Rafiee and assisted in writing two of the group's papers, titled "Deriving the Turnover Frequency of Aminoxyl-Catalyzed Alcohol Oxidation by Chronoamperometry: An Introduction to Organic Electrocatalysis" and "Constant Potential and Constant Current Electrolysis: An Introduction and Comparison of Different Techniques for Organic Electrosynthesis" in 2021.